Lepton-nucleus interaction using QMC based approaches

Noemi Rocco

NuFact 2024 - The 25th International Workshop on Neutrinos from Accelerators
ANL— Sept 16 - 21, 2024

Outline

- Lepton - nucleus interactions : GFMC
- Lepton - nucleus interactions : Factorization Scheme
- Lepton - nucleus interactions : BSM scenarios
  - Bayesian Artificial Neural network

Noemi Rocco, nrocco@fnal.gov

Ab initio Methods

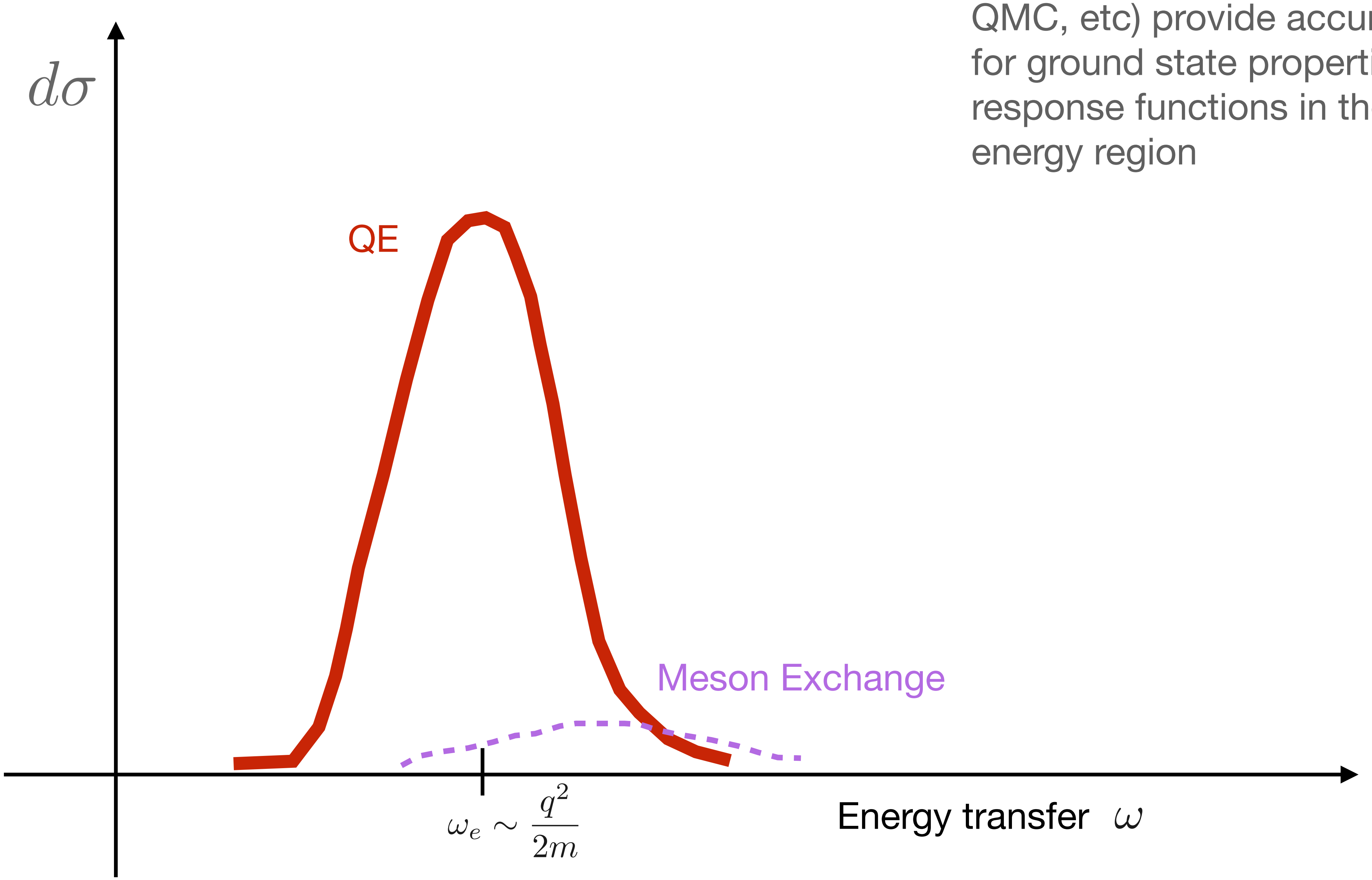

Ab-initio methods (CC, IMSRG, SCGF, QMC, etc) provide accurate predictions for ground state properties of nuclei + response functions in the low/moderate energy region

Noemi Rocco, nrocco@fnal.gov

Many-Body method: GFMC

QMC techniques **projects out the exact lowest-energy state:** $e^{-(H-E_0)\tau}|\Psi_T\rangle \to |\Psi_0\rangle$

Nuclear response function involves evaluating a number of transition amplitudes.
Valuable information can be obtained from the **integral transform of the response function**

$$E_{\alpha\beta}(\sigma,\mathbf{q}) = \int d\omega K(\sigma,\omega) R_{\alpha\beta}(\omega,\mathbf{q}) = \langle\psi_0|J_\alpha^\dagger(\mathbf{q}) K(\sigma, H-E_0) J_\beta(\mathbf{q})|\psi_0\rangle$$

Inverting the Laplace transform is a complicated problem

A. Lovato et al, PRL117 (2016), 082501, PRC97 (2018), 022502

— electron-^{4}He scattering

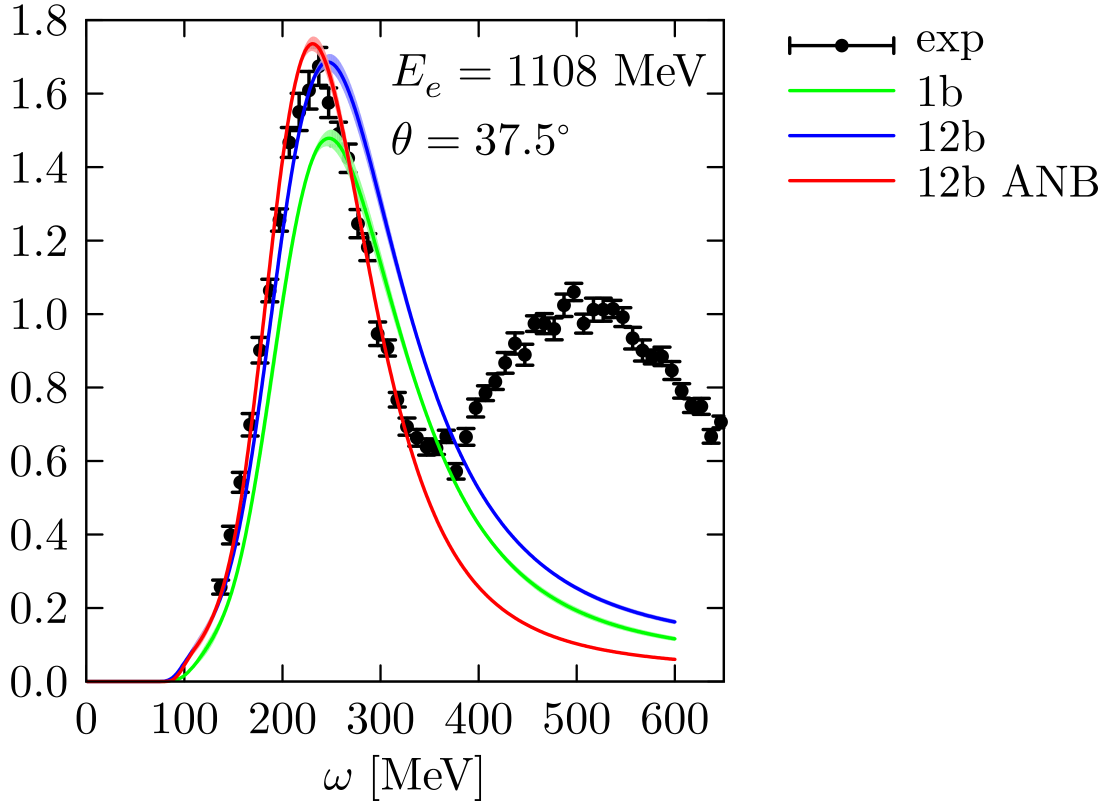

Inclusive results which are virtually correct in the QE

Different Hamiltonians can be used in the time-evolution operator

Relies on non-relativistic treatment of the kinematics

Can not handle explicit pion degrees of freedom

Noemi Rocco, nrocco@fnal.gov

Axial form factor determination

- Alternative derivation based on **z-expansion** —model independent parametrization

$$F_A(q^2) = \sum_{k=0}^{k_{\max}} a_k z(q^2)^k,$$

known functions

free parameters

Bhattacharya, Hill, and Paz PRD 84 (2011) 073006

A.S.Meyer et al, Phys.Rev.D 93 (2016) 11, 113015

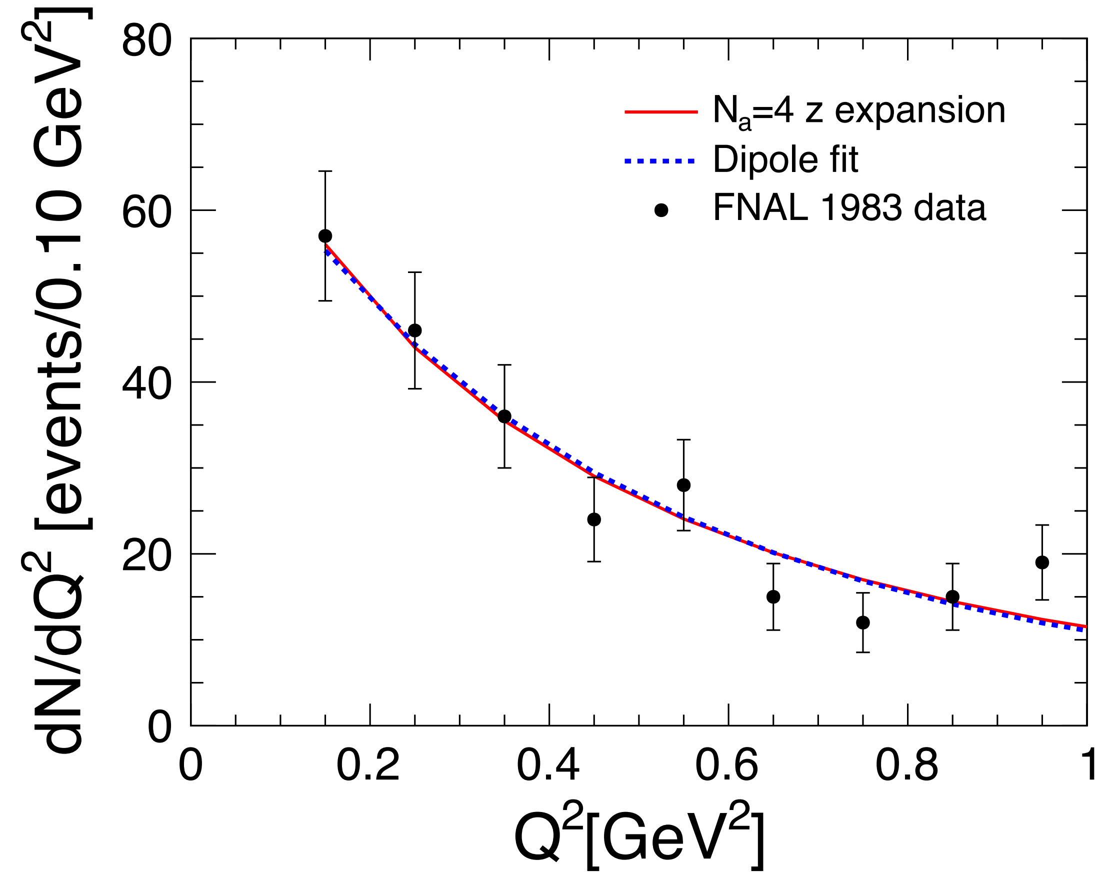

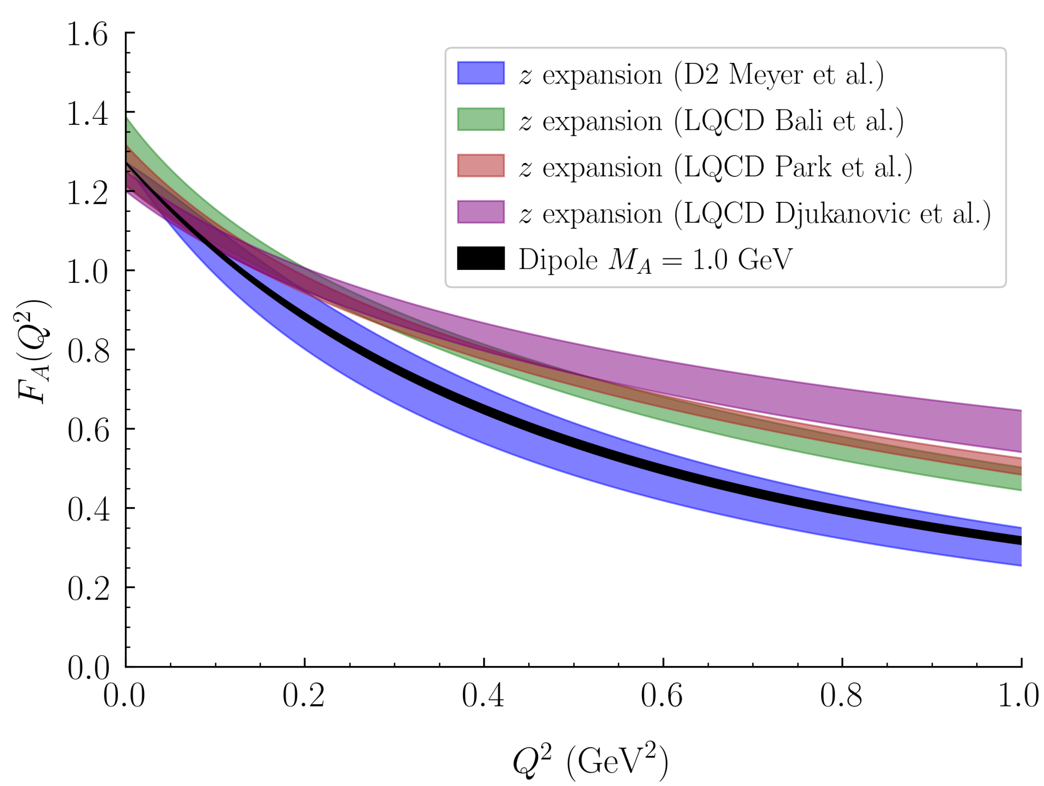

D2 Meyer et al: fits to neutrino-deuteron scattering data

LQCD result: general agreement between the different calculations

LQCD results are 2-3σ larger than D2 Meyer ones for $Q^2 > 0.3$ GeV^2

Study of model dependence in neutrino predictions

MiniBooNE results; study of the dependence on the axial form factor:

D.Simons, N. Steinberg, NR, et al arXiv:2210.02455

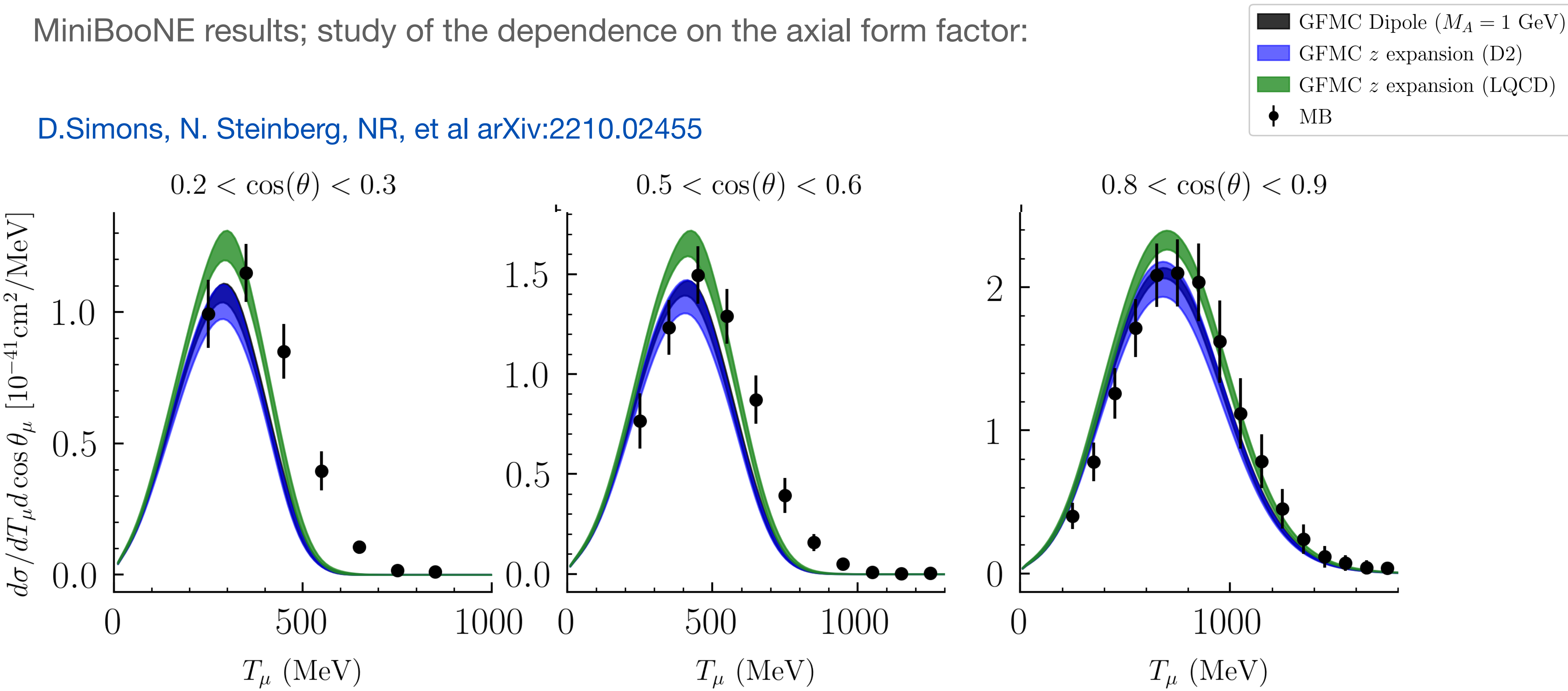

D.Simons, N. Steinberg et al, 2210.02455

MiniBooNE	$0.2 < \cos\theta_\mu < 0.3$	$0.5 < \cos\theta_\mu < 0.6$	$0.8 < \cos\theta_\mu < 0.9$
GFMC Difference in $d\sigma_{\text{peak}}$ (%)	18.6	17.1	12.2

Noemi Rocco, nrocco@fnal.gov

Study of model dependence in neutrino predictions

T2K results; study of the dependence on the axial form factor:

D.Simons, N. Steinberg, NR, et al arXiv:2210.02455

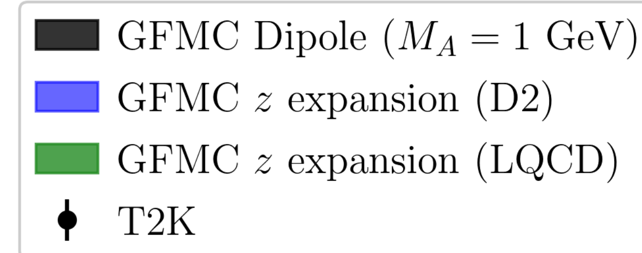

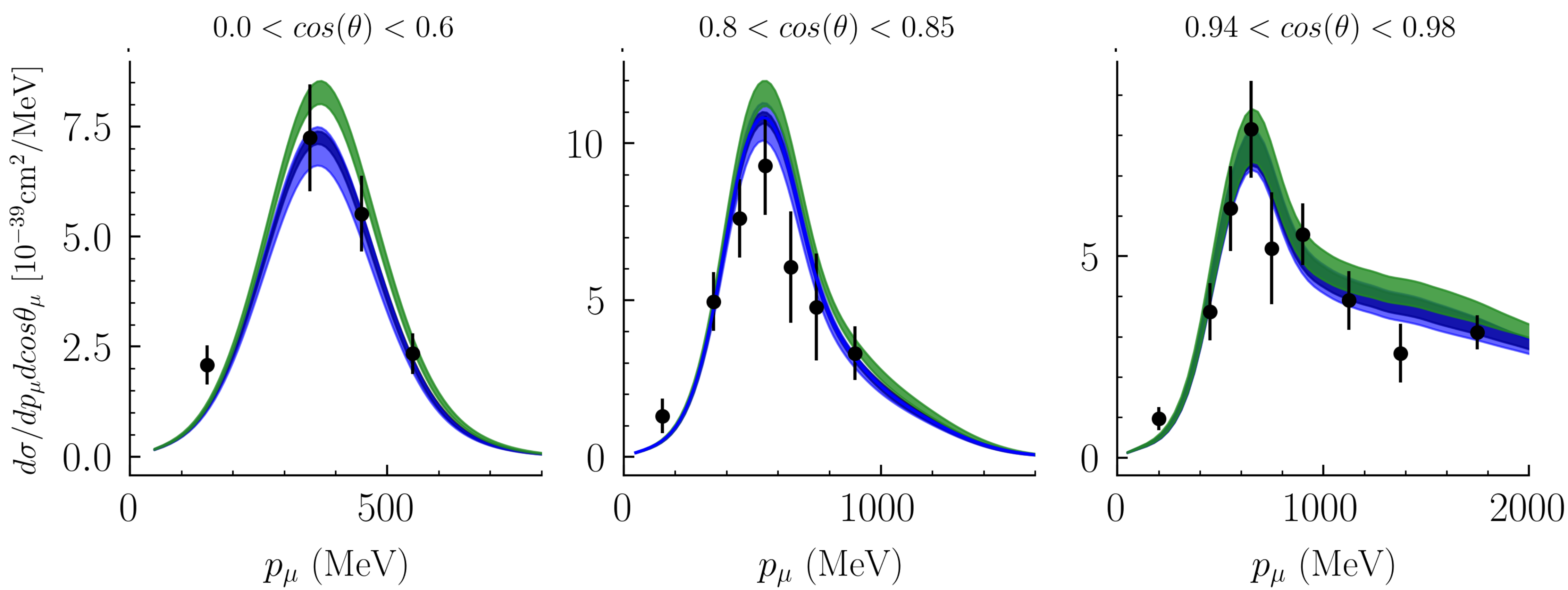

D.Simons, N. Steinberg et al, 2210.02455

T2K	$0.0 < \cos\theta_\mu < 0.6$	$0.80 < \cos\theta_\mu < 0.85$	$0.94 < \cos\theta_\mu < 0.98$
GFMC difference in $d\sigma_{\mathrm{peak}}$ (%)	15.8	8.0	4.6

Noemi Rocco, nrocco@fnal.gov

Cross sections: Green's Function Monte Carlo

MiniBooNE results including relativistic corrections

A.Nikolakopoulos, A.Lovato, NR, PRC 109 (2024) 1, 014623

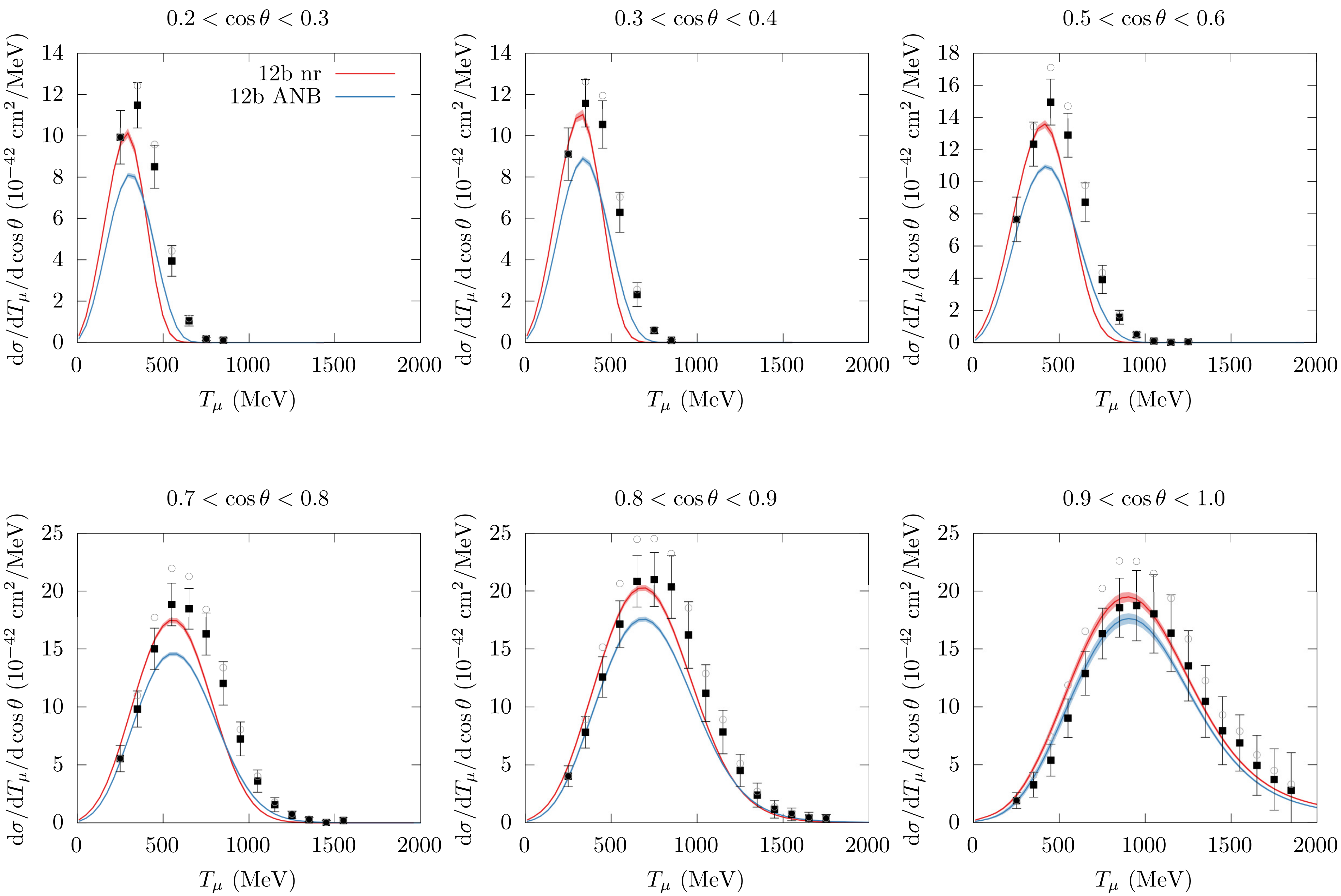

Noemi Rocco, nrocco@fnal.gov

Relevant Inputs from AFDMC

The AFDMC method uses a spin-isospin basis given by the outer product of single-nucleon spinors

$$|S\rangle = |s_1\rangle \otimes |s_2\rangle \cdots \otimes |s_A\rangle \quad \longleftrightarrow \quad |s\rangle = s_{p\uparrow}|p\uparrow\rangle + s_{p\downarrow}|p\downarrow\rangle + s_{n\uparrow}|n\uparrow\rangle + s_{n\downarrow}|n\downarrow\rangle$$

This allows us to use QMC techniques to describe larger nuclei like ^{16}O and ^{40}Ca

AFDMC point nucleon density of ^{16}O compared with the CVMC method

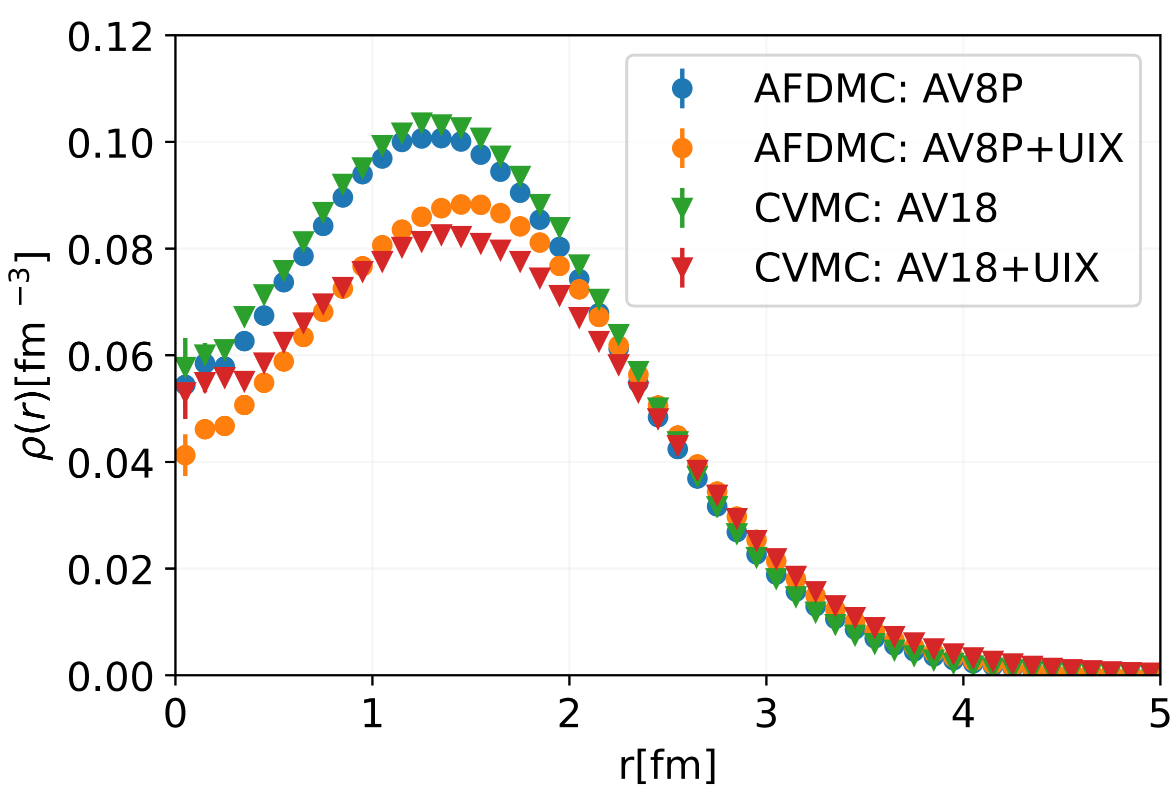

Nucleon momentum distribution of ^{16}O compared with the CVMC method

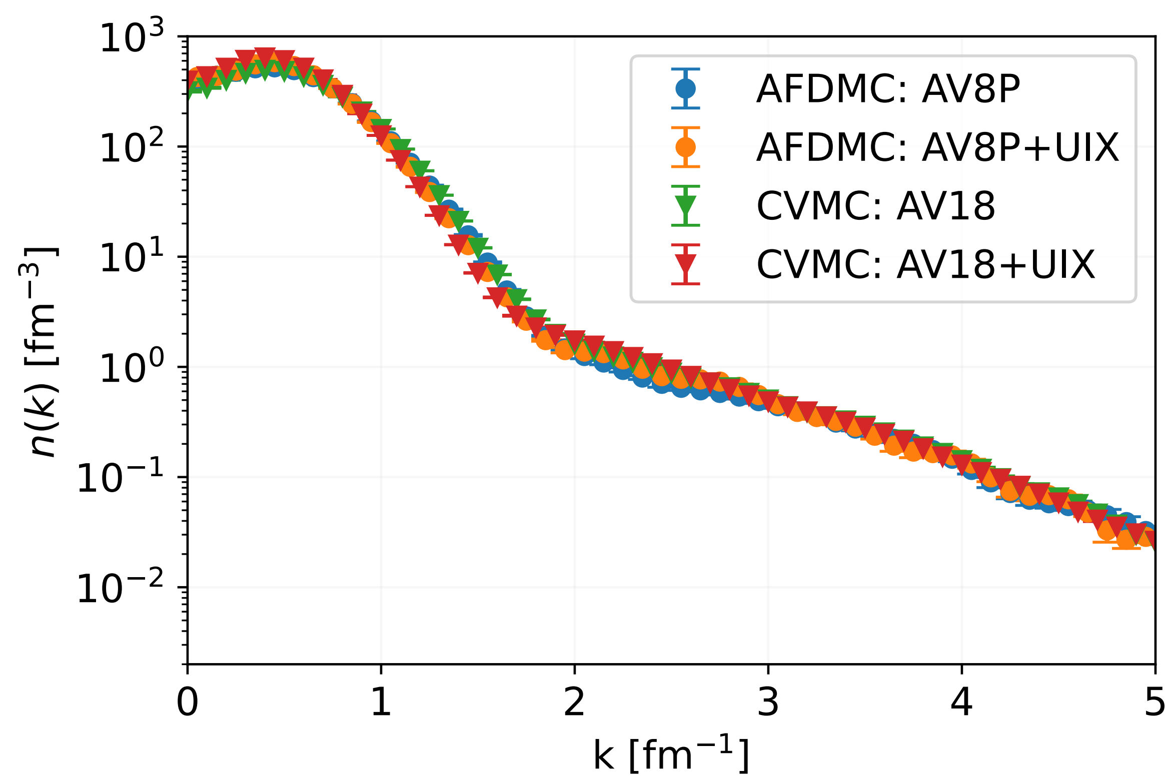

Noemi Rocco, nrocco@fnal.gov

Relevant Inputs from AFDMC

Wigner Functions give the joint quasi-probability distribution of finding a nucleon with **k** and **r** in the nucleus

Wigner distributions provide insight on the momentum structure of nuclear radii and spatial structure of the kinetic energy and what is the role of SRC.

$$w(\mathbf{r},\mathbf{k}) = \frac{1}{(2\pi)^3}\int d\mathbf{x} e^{i\mathbf{k}\cdot\mathbf{x}} \left| \mathbf{r} + \frac{\mathbf{x}}{2} \right\rangle \left\langle \mathbf{r} - \frac{\mathbf{x}}{2} \right| = \frac{1}{(2\pi)^3}\int d\mathbf{x} e^{-i\mathbf{q}\cdot\mathbf{r}} \left| \mathbf{k} + \frac{\mathbf{q}}{2} \right\rangle \left\langle \mathbf{k} - \frac{\mathbf{q}}{2} \right|$$

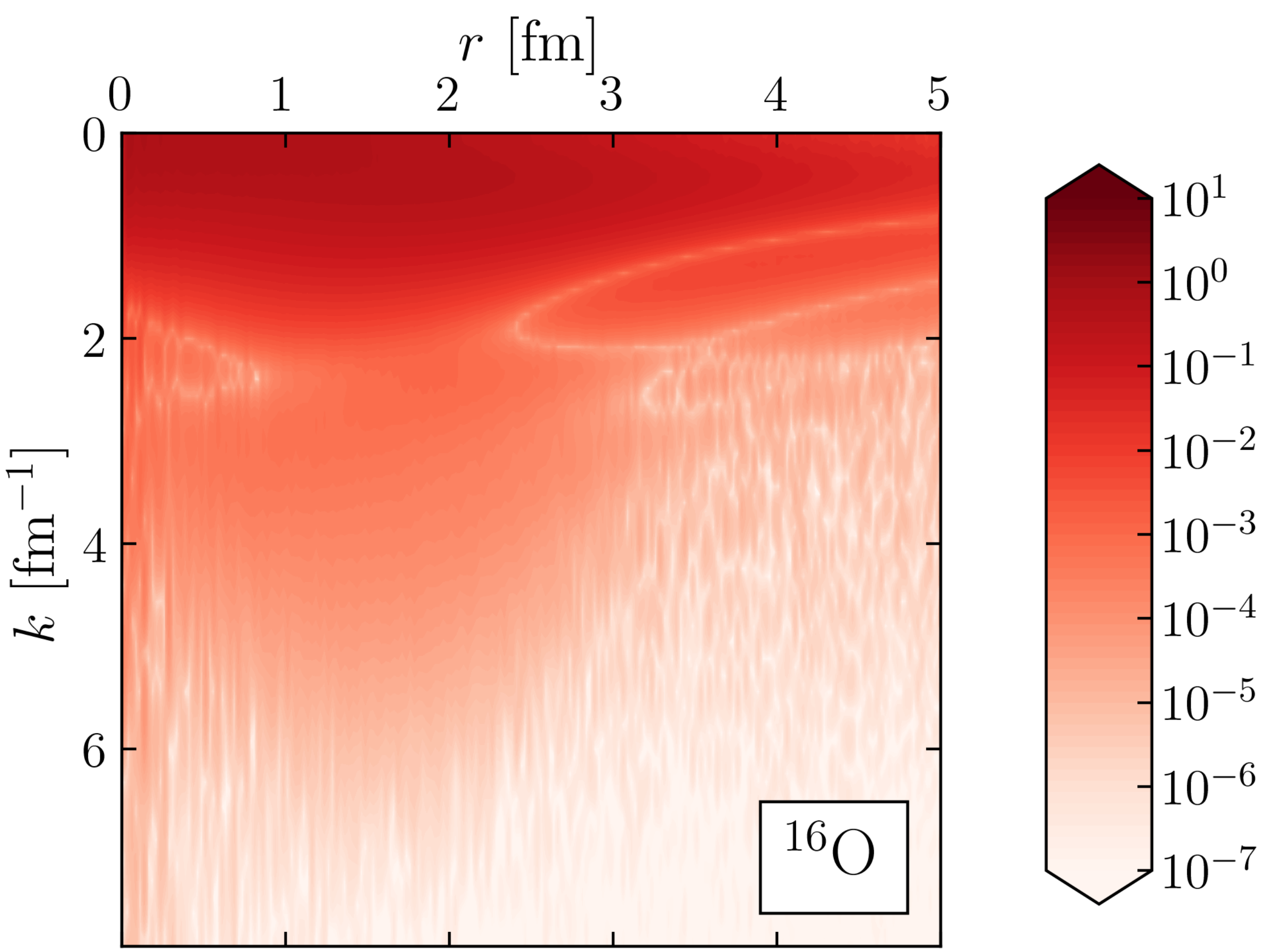

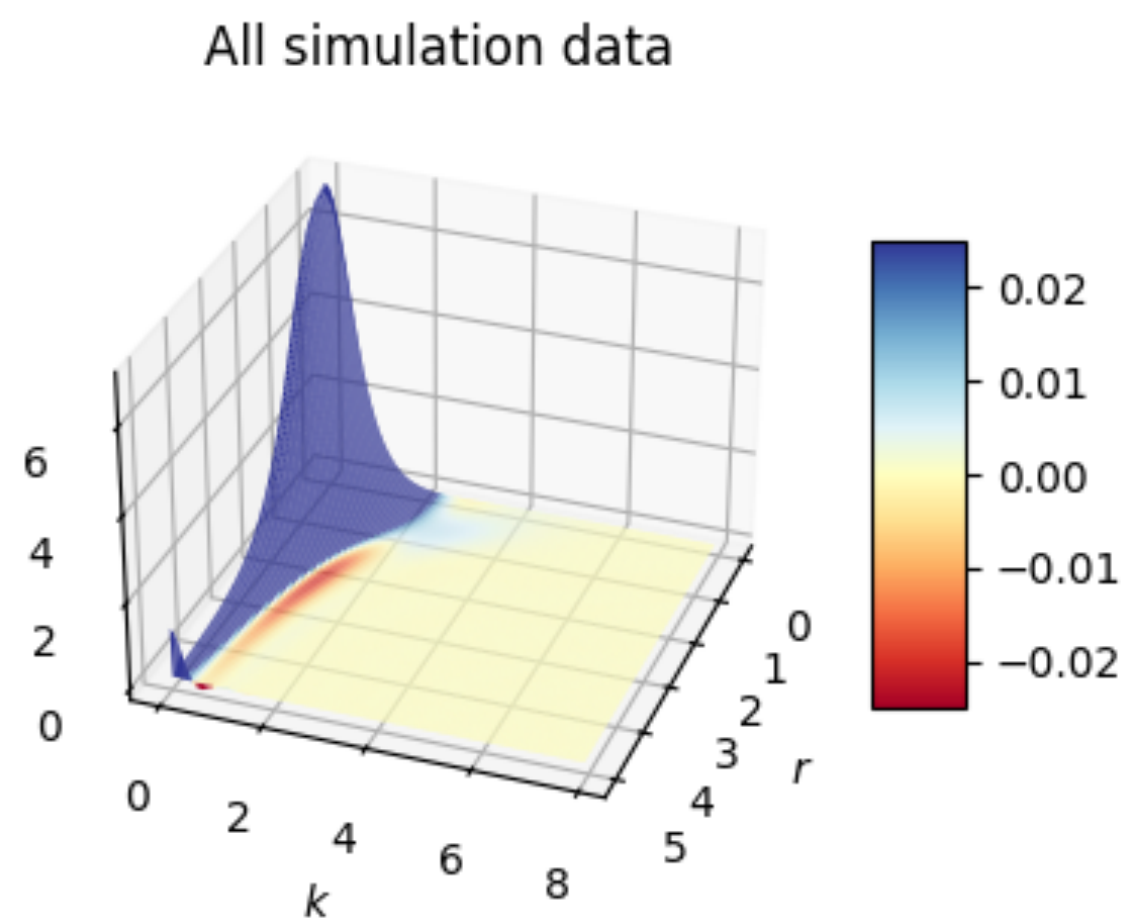

Noemi Rocco, nrocco@fnal.gov

Factorization Based Approaches

Factorization of the hadronic final states: allows to tackle exclusive channels + higher energies relevant for DUNE

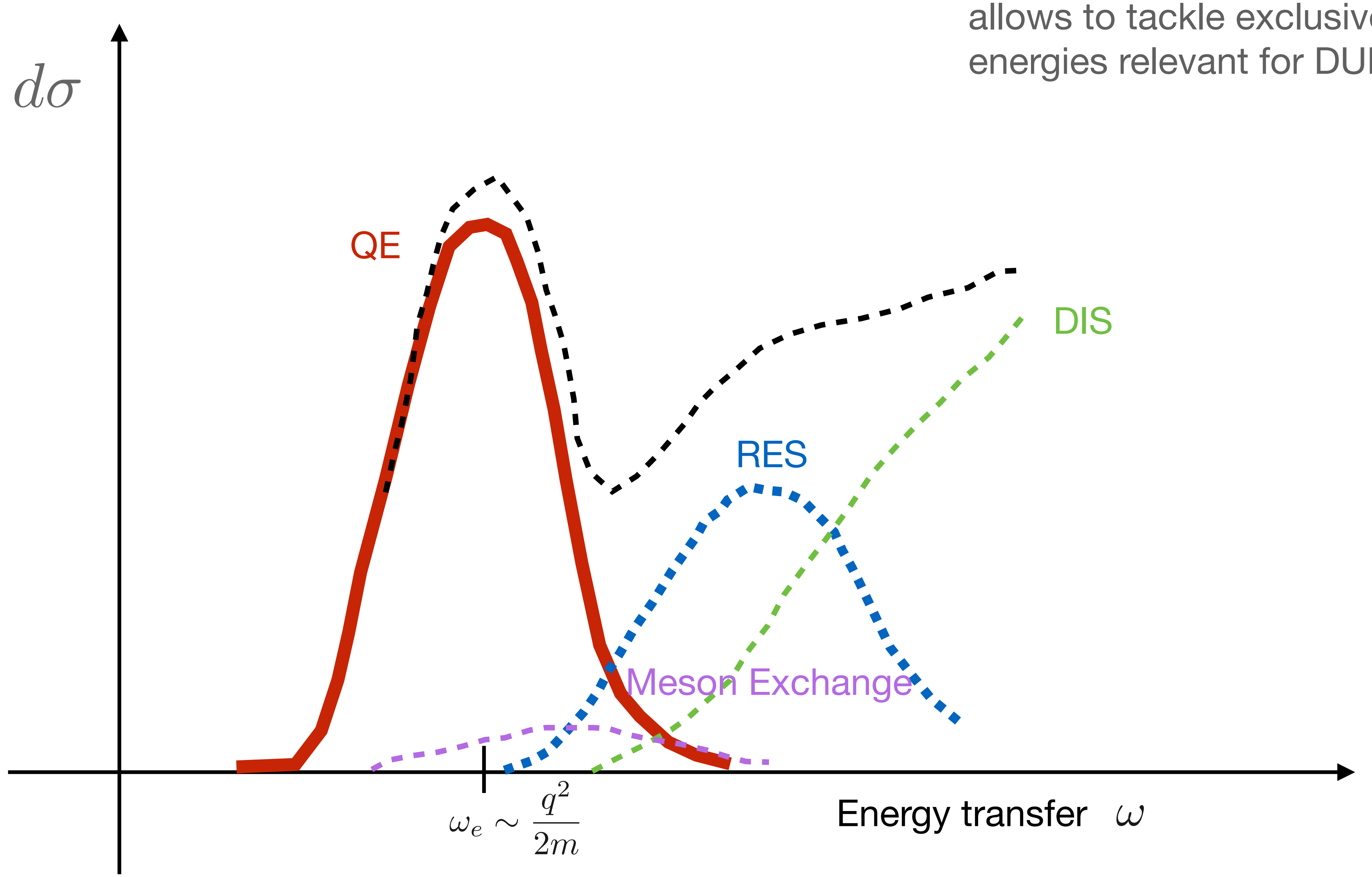

Noemi Rocco, nrocco@fnal.gov
Fermilab

Spectral function approach

At large momentum transfer, the scattering reduces to the sum of individual terms

$$J_\alpha = \sum_i j^i_\alpha \qquad\qquad |\Psi_f\rangle \to |p\rangle \otimes |\Psi_f\rangle_{A-1}$$

The incoherent contribution of the one-body response reads

$$R_{\alpha\beta} \simeq \int \frac{d^3k}{(2\pi)^3} dE P_h(\mathbf{k}, E) \sum_i \langle k|{j^i_\alpha}^\dagger|k+q\rangle\langle k+q|j^i_\beta|k\rangle \delta(\omega + E - e(\mathbf{k}+\mathbf{q}))$$

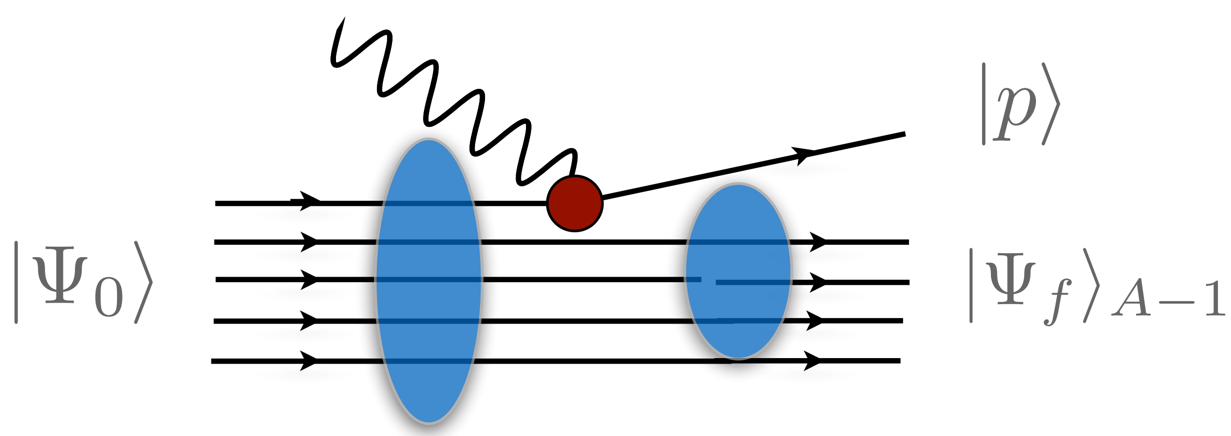

The Spectral Function is the imaginary part of the two point Green's Function

Different many-body methods can be adopted to determine it

O. Benhar et al, Rev.Mod.Phys. 80 (2008)

I. Korover, et al Phys.Rev.C 107 (2023) 6, L061301

***NR*, Frontiers in Phys. 8 (2020) 116**

J.E. Sobczyk et al, PRC 106 (2022) 3

J.E. Sobczyk et al, PRC 109 (2024)

QMC Spectral function of light nuclei

- Single-nucleon spectral function:

$$P_{p,n}(\mathbf{k},E) = \sum_n \left| \langle \Psi_0^A | [|k\rangle \otimes |\Psi_n^{A-1}\rangle] \right|^2 \delta(E + E_0^A - E_n^{A-1}) = P^{MF}(\mathbf{k},E) + P^{\rm corr}(\mathbf{k},E)$$

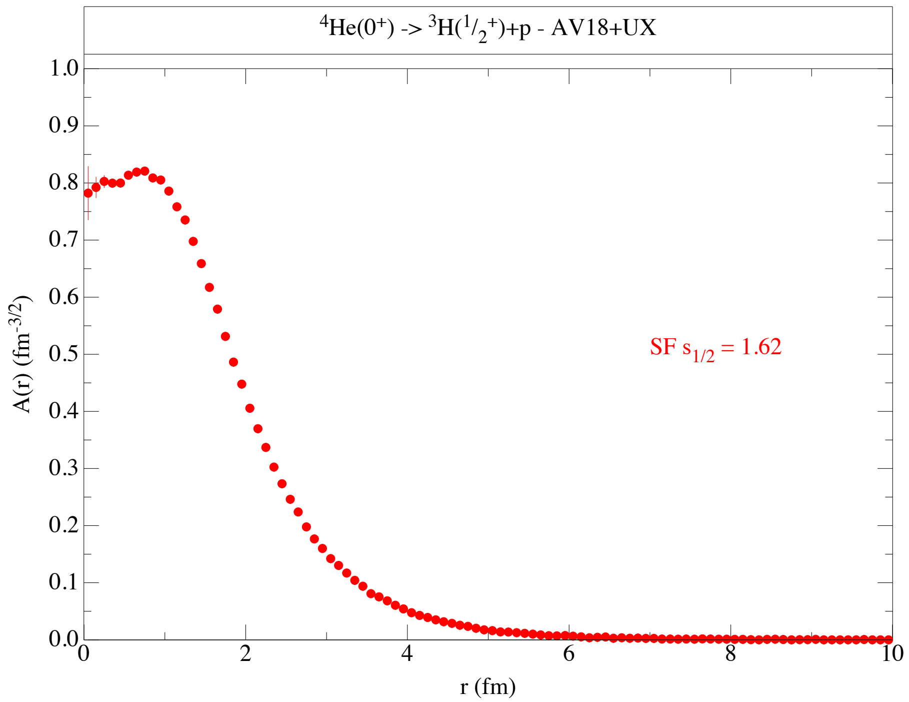

$$P^{MF}(\mathbf{k},E) = \left| \langle \Psi_0^A | [|k\rangle \otimes |\Psi_n^{A-1}\rangle] \right|^2 \times \delta\left(E - B_A + B_{A-1} - \frac{\mathbf{k}^2}{2m_{A-1}}\right)$$

- The single-nucleon overlap has been computed within VMC (center of mass motion fully accounted for)

$$P^{\rm corr}(\mathbf{k},E) = \int d^3k' \left| \langle \Psi_0^A | [|k\rangle |k'\rangle \otimes |\Psi_n^{A-2}\rangle] \right|^2 \times \delta\left(E - B_A - e(\mathbf{k}') + B_{A-2} - \frac{(\mathbf{k}+\mathbf{k}')^2}{2m_{A-2}}\right)$$

- Written in terms of two-body momentum distribution

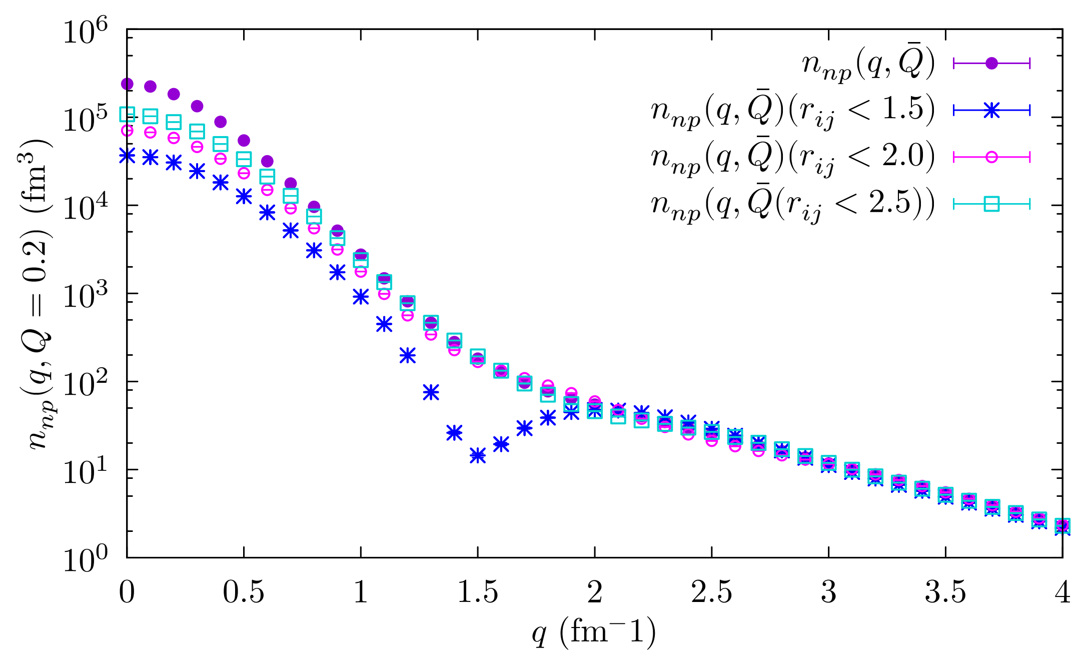

Noemi Rocco, nrocco@fnal.gov
Fermilab

Spectral function approach

$$\boxed{|f\rangle \rightarrow |pp'\rangle_a \otimes |f_{A-2}\rangle}$$

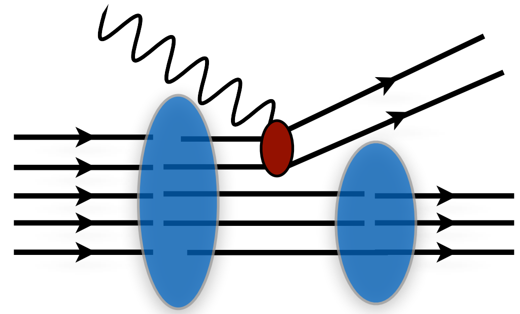

The hadronic tensor for two-body current factorizes as

$$R^{\mu\nu}_{2b}(\mathbf{q},\omega) \propto \int dEd^3kd^3k' P_{2b}(\mathbf{k},\mathbf{k}',E) \times d^3pd^3p' |\langle kk'|j^\mu_{2b}|pp'\rangle|^2$$

$$\boxed{|f\rangle \rightarrow |p_\pi p\rangle \otimes |f_{A-1}\rangle}$$

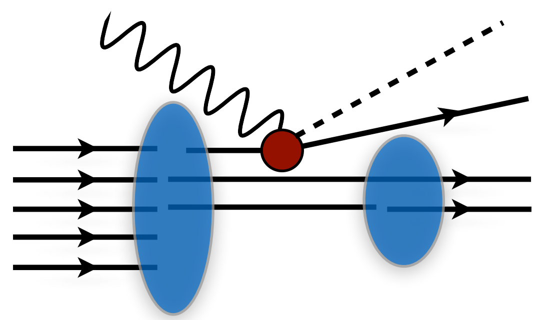

Production of real π in the final state

$$R^{\mu\nu}_{1b\pi}(\mathbf{q},\omega) \propto \int dEd^3kP_{1b}(\mathbf{k},E) \times d^3pd^3k_\pi |\langle k|j^\mu|pk_\pi\rangle|^2$$

* Pion production elementary amplitudes currently derived within the extremely sophisticated **Dynamic Couple Chanel approach**;

S.X.Nakamura, et al PRD92(2015)
T. Sato, et al PRC67(2003)

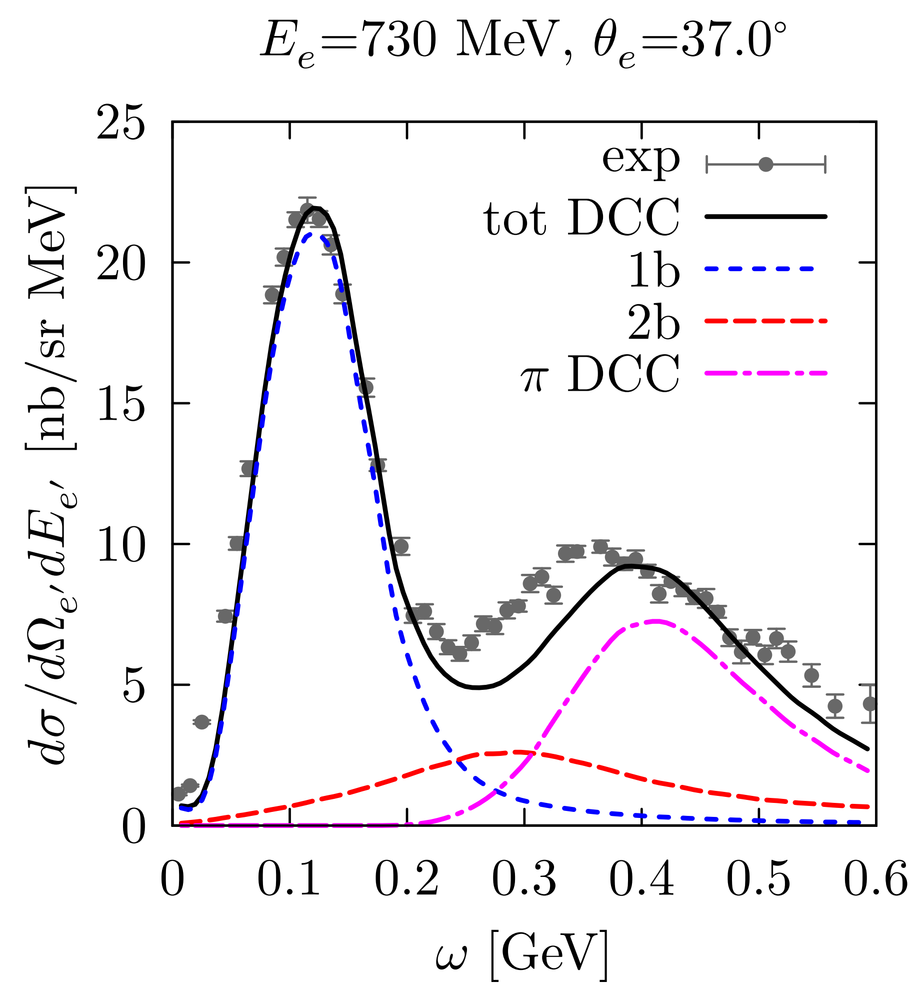

***NR,* Frontiers in Phys. 8 (2020) 116**

Noemi Rocco, nrocco@fnal.gov

Axial Form Factors Uncertainty needs

D.Simons, N. Steinberg et al, 2210.02455

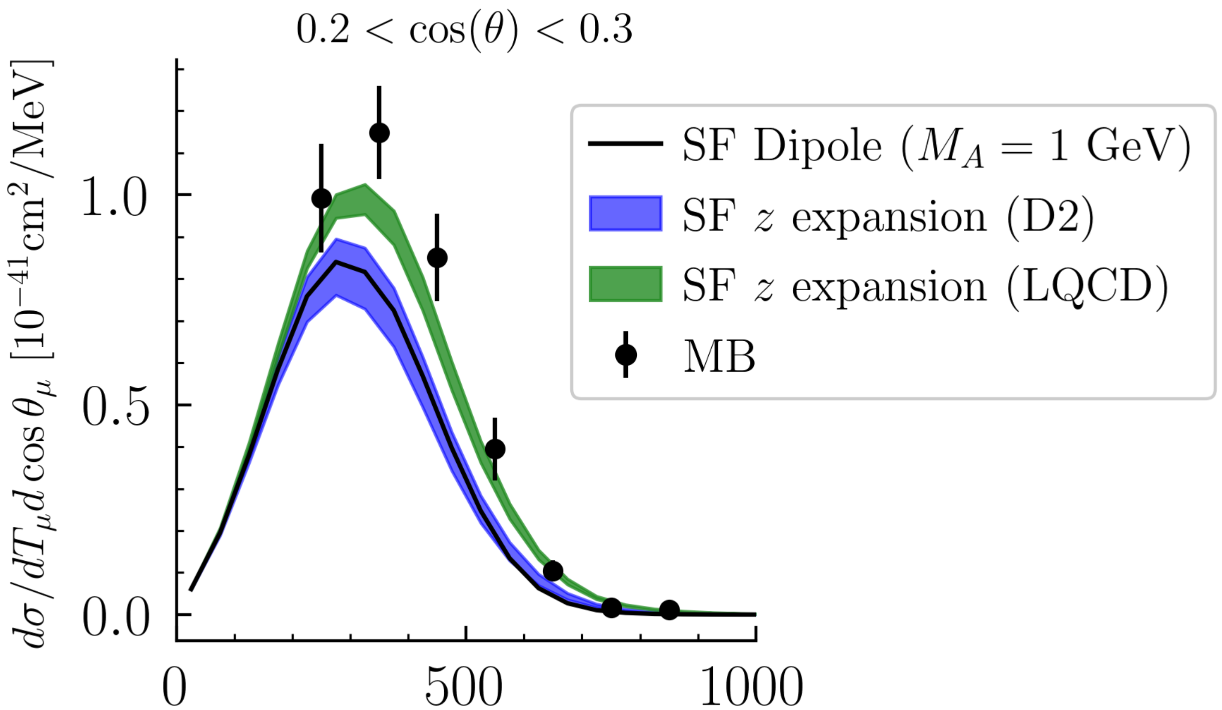

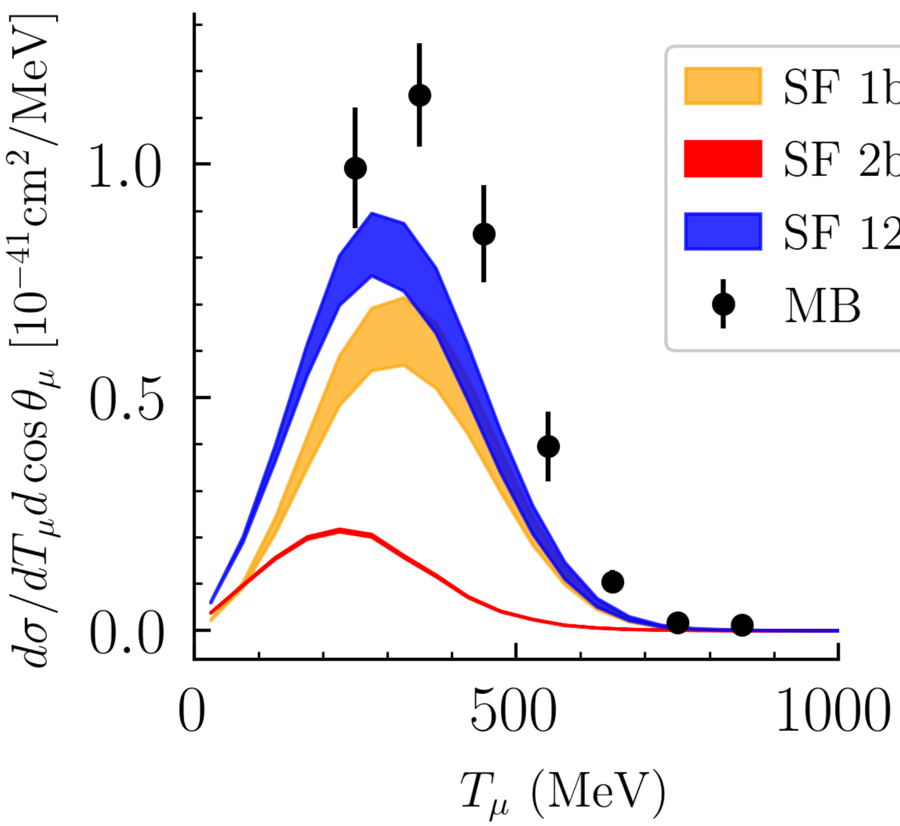

✴ Axial form factor dependence:

MiniBooNE	$0.2 < \cos\theta_\mu < 0.3$
SF Difference in $d\sigma_{\mathrm{peak}}$ (%)	16.3

✴ Many-body method dependence:

MiniBooNE	$0.2 < \cos\theta_\mu < 0.3$
GFMC/SF difference in $d\sigma_{\mathrm{peak}}$ (%)	22.8

Noemi Rocco, nrocco@fnal.gov
Fermilab

Resonance Uncertainty needs

The largest contributions to two-body currents arise from resonant $N \rightarrow \Delta$ transitions yielding pion production

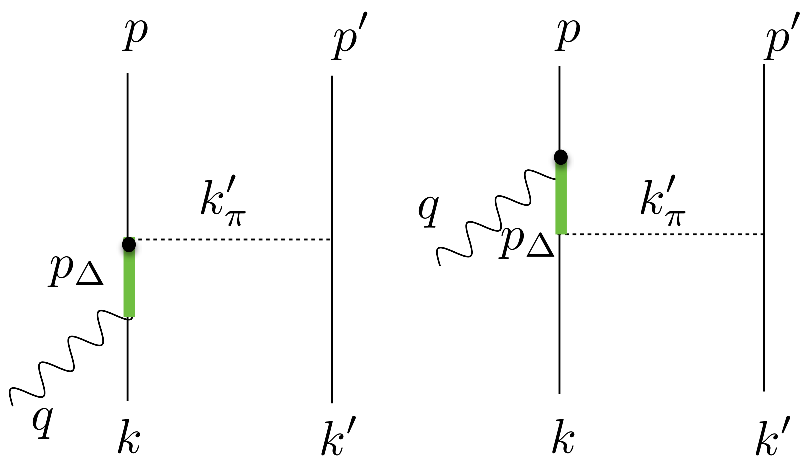

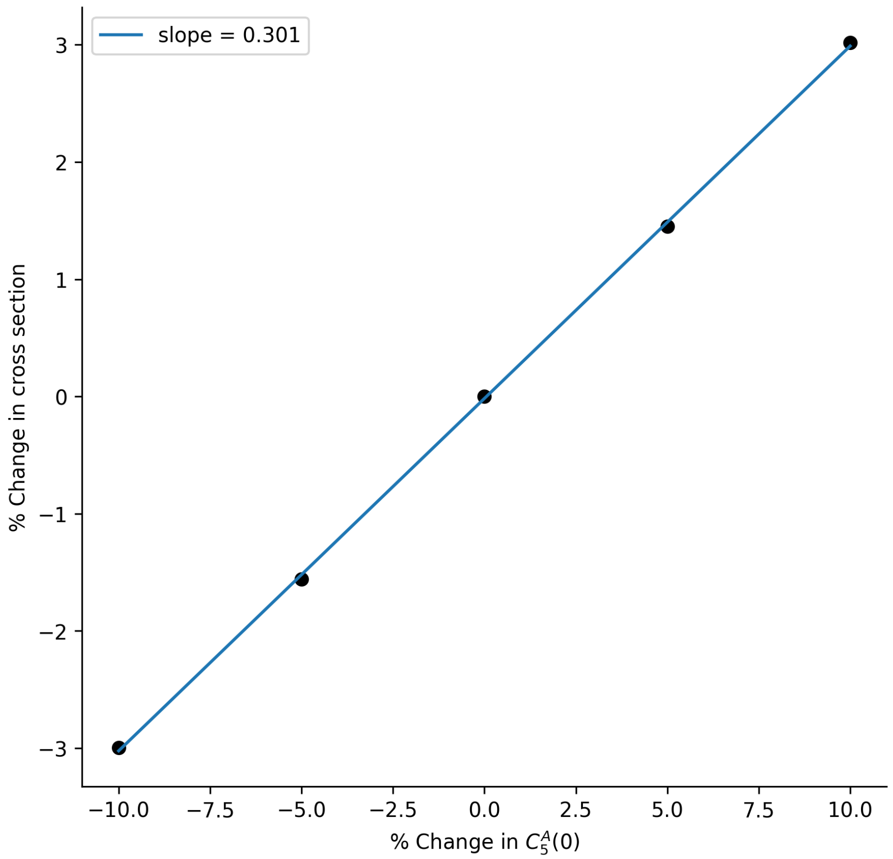

D.Simons, N. Steinberg et al, 2210.02455

The normalization of the dominant $N \rightarrow \Delta$ transition form factor needs be known to 3% precision to achieve 1% cross-section precision for MiniBooNE kinematics

State-of-the-art determinations of this form factor from experimental data on pion electroproduction achieve 10-15% precision (under some assumptions)

Hernandez et al, PRD 81 (2010)

Further constraints on $N \rightarrow \Delta$ transition relevant for two-body currents and π production will be necessary to achieve few-percent cross-section precision

Including the one- and two-body interference

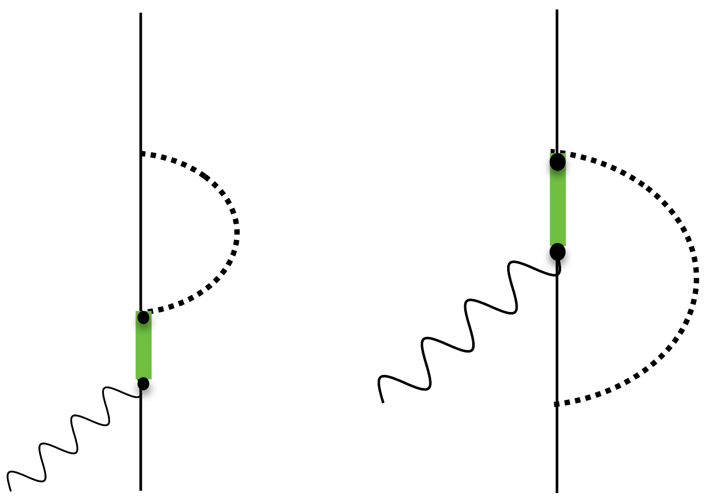

We recently included interference effects between one- and two-body currents yielding single nucleon knock-out

Observe a small quenching in the longitudinal channel and an enhancement in the q.e. peak in the transverse → agreement with the GFMC

N. Steinberg, NR, A. Lovato, arXiv: 2312.12545

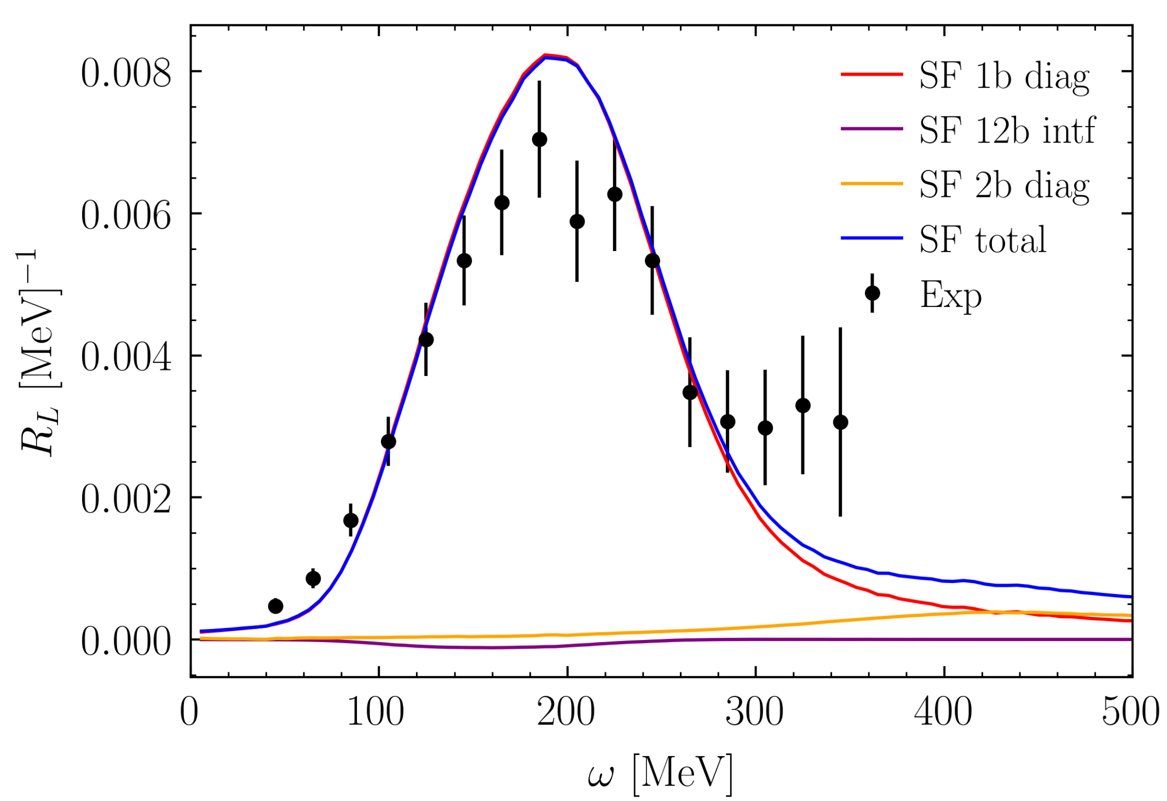

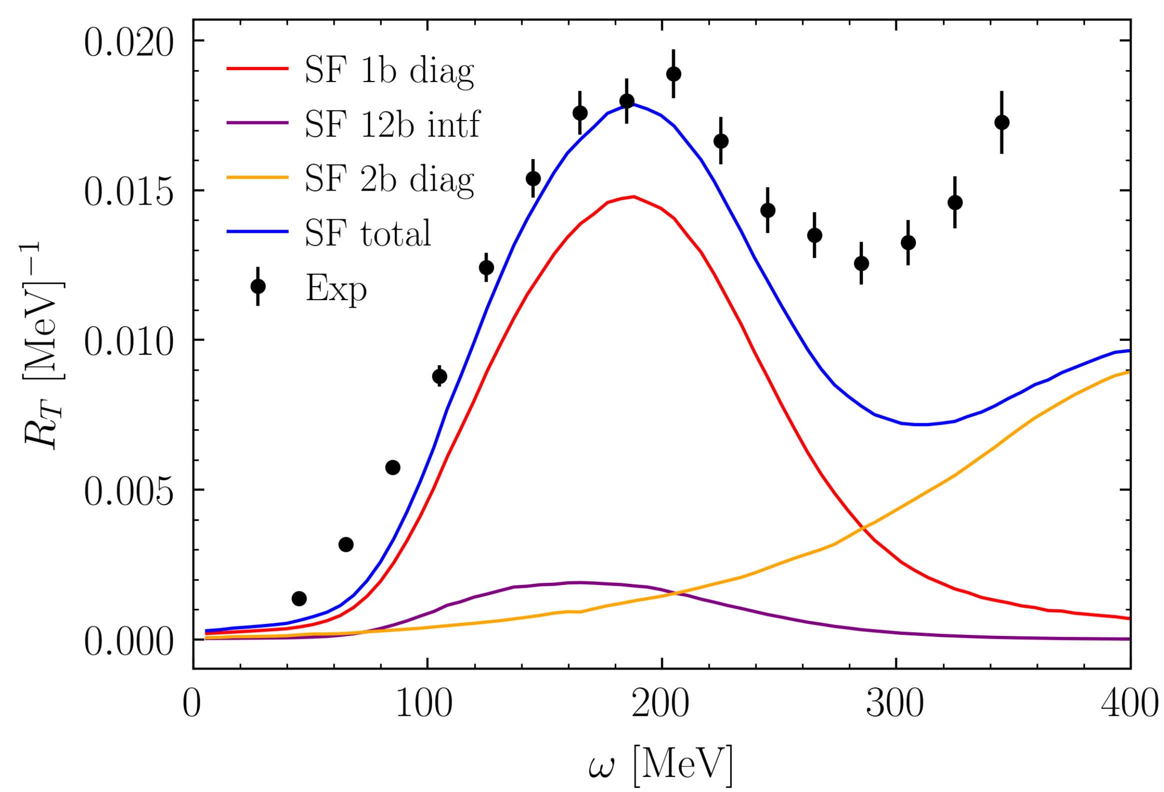

Including the one- and two-body interference

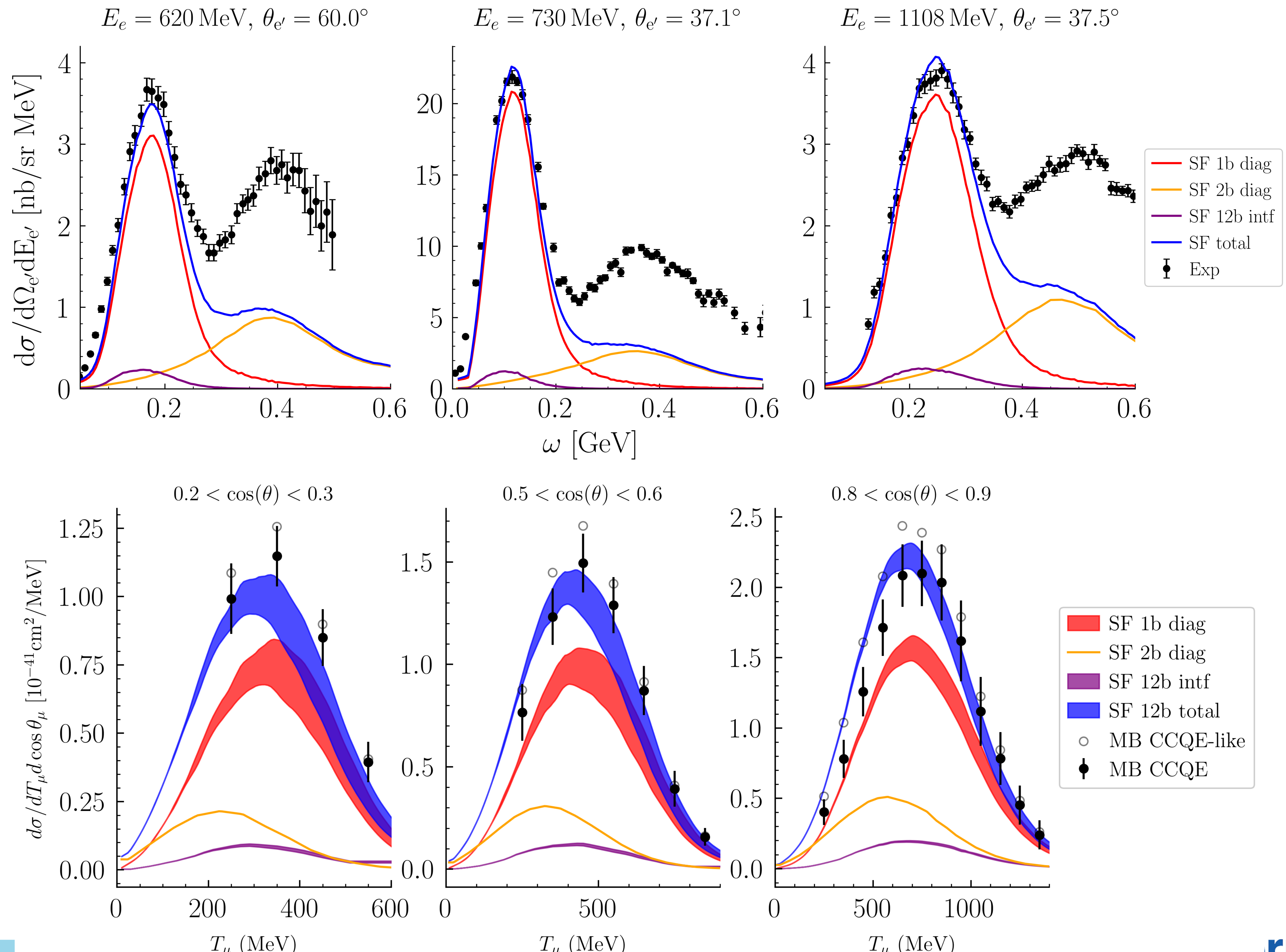

Noemi Rocco, nrocco@fnal.gov

N. Steinberg, NR, A. Lovato, arXiv: 2312.12545

Interplay with BSM scenarios

Z. Tabrizi, J. Kopp, NR, JHEP 08 (2024) 187

- Interested in Weak Effective Field Theory (WEFT), valid below the electroweak scale, with the electroweak gauge bosons, the Higgs boson, and the top quark integrated out

- CC: New left/right handed, (pseudo)scalar and tensor interactions

$$\begin{aligned}\mathcal{L}_{\text{WEFT}} \supset\ & -\frac{2V_{ud}}{v^2}\Big\{ [\mathbf{1}+\epsilon_L]_{\alpha\beta}\,(\bar{u}\gamma^\mu P_L d)(\bar{\ell}_\alpha\gamma_\mu P_L\nu_\beta) \\ & +[\epsilon_R]_{\alpha\beta}(\bar{u}\gamma^\mu P_R d)(\bar{\ell}_\alpha\gamma_\mu P_L\nu_\beta) \\ & +\frac{1}{2}[\epsilon_S]_{\alpha\beta}(\bar{u}d)(\bar{\ell}_\alpha P_L\nu_\beta)-\frac{1}{2}[\epsilon_P]_{\alpha\beta}(\bar{u}\gamma_5 d)(\bar{\ell}_\alpha P_L\nu_\beta) \\ & +\frac{1}{4}[\hat{\epsilon}_T]_{\alpha\beta}(\bar{u}\sigma^{\mu\nu}P_L d)(\bar{\ell}_\alpha\sigma_{\mu\nu}P_L\nu_\beta)+\text{h.c.}\Big\}\end{aligned}$$

- SM Interactions:

V : $$\langle p(p_p)|\bar{q}_u\gamma_\mu q_d|n(p_n)\rangle = \bar{u}_p(p_p)\Big[G_V(Q^2)\gamma_\mu + i\frac{\tilde{G}_{T(V)}(Q^2)}{2M_N}\sigma_{\mu\nu}q^\nu - \cancel{\frac{\tilde{G}_S(Q^2)}{2M_N}}q_\mu\Big]u_n(p_n)$$

A : $$\langle p(p_p)|\bar{q}_u\gamma_\mu\gamma_5 q_d|n(p_n)\rangle = \bar{u}_p(p_p)\Big[G_A(Q^2)\gamma_\mu\gamma_5 + i\cancel{\frac{\tilde{G}_{T(A)}(Q^2)}{2M_N}}\sigma_{\mu\nu}q^\nu\gamma_5 - \frac{\tilde{G}_P(Q^2)}{2M_N}q_\mu\gamma_5\Big]u_n(p_n)$$

Form factors - new interactions

Z. Tabrizi, J. Kopp, NR, arxiv: 2401.07902

- Scalar: conservation of the vector current (CVC)

$$G_S(Q^2) = -\frac{\delta M_N^{QCD}}{\delta m_q} G_V(Q^2) + \frac{Q^2/2M_N}{\delta m_q} \tilde{G}_S(Q^2)$$

small

- Partially-conserved axial current (PCAC)

$$G_P(Q^2) = \frac{M_N}{m_q} G_A(Q^2) + \frac{Q^2/2M_N}{2m_q} \tilde{G}_P(Q^2)$$

- Tensor: LQCD and theoretical considerations

We can not neglect $\tilde{G}_S(Q^2)$ anymore.

We analyze for the first time how the **axial form factor uncertainty affects the study of new interactions** beyond the SM and we find a sizable effect

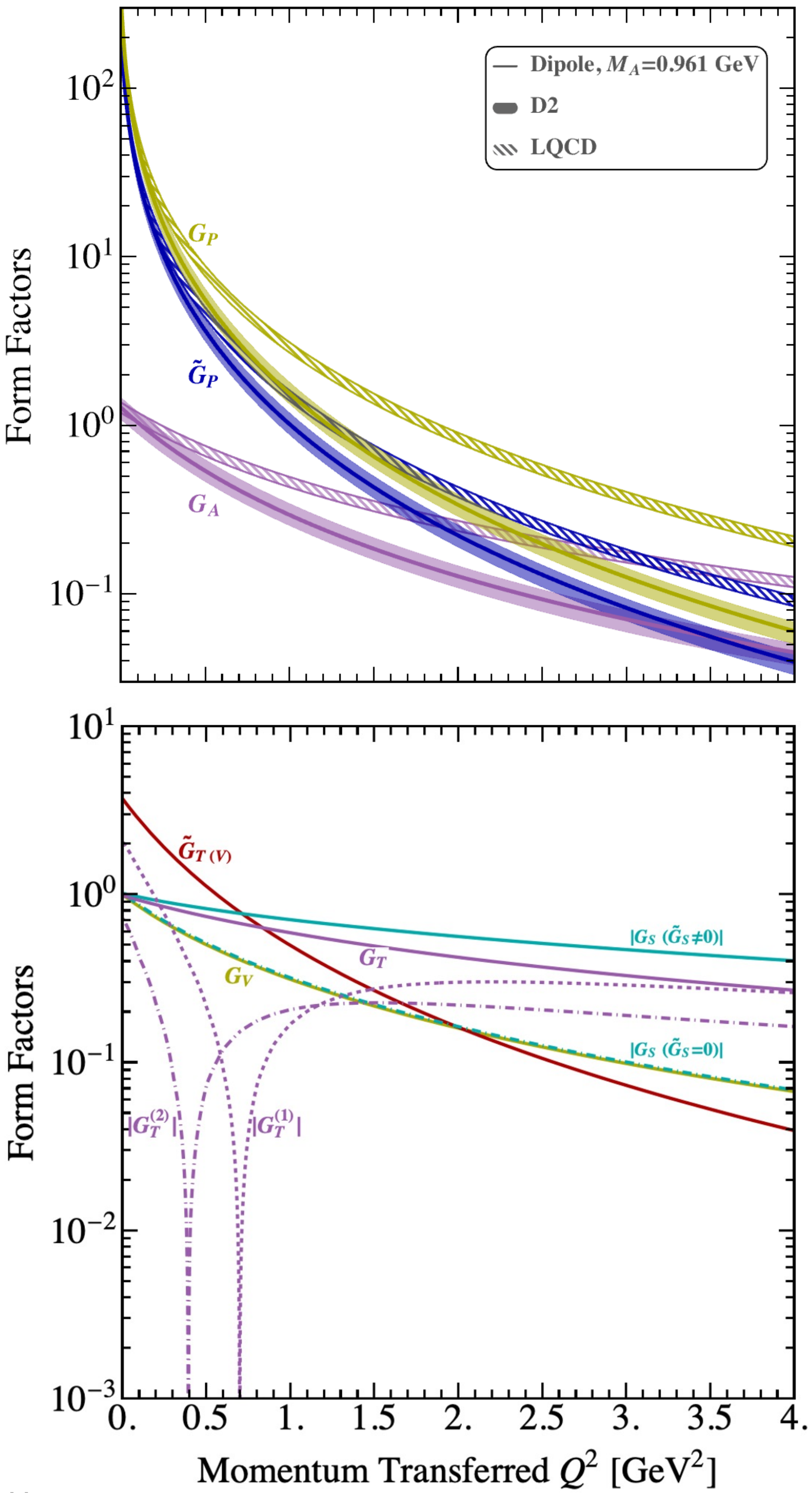

 Noemi Rocco, nrocco@fnal.gov

Interplay with BSM scenarios

Z. Tabrizi, J. Kopp, NR, arxiv: 2401.07902

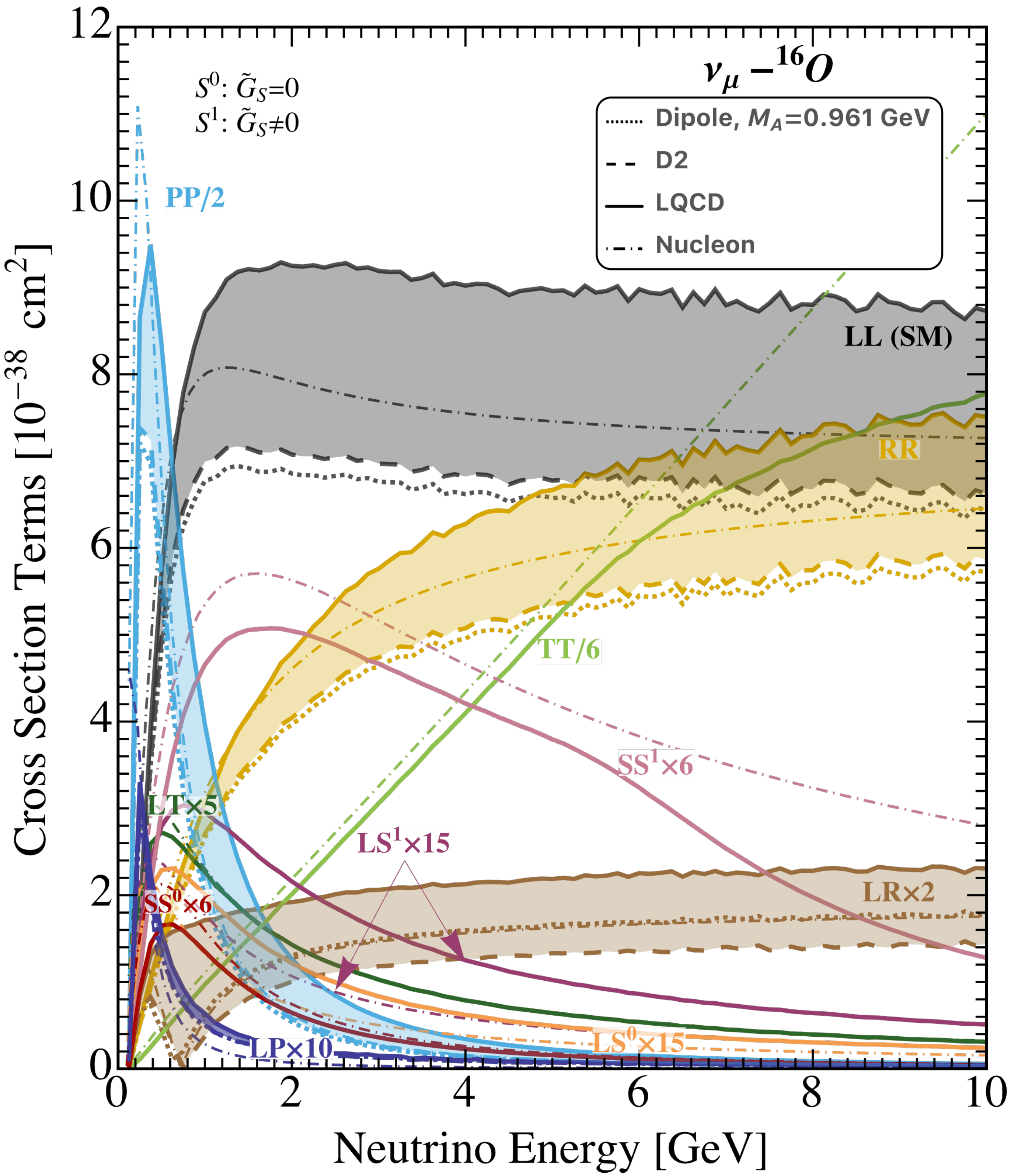

- The pseudoscalar and tensor interactions, exhibit cross sections notably enhanced compared to those of the Standard Model. {there is a considerable margin of uncertainty}
- The axial form factor introduces significant systematic uncertainties, true for both SM and BSM interactions
- Nuclear effects are crucial even at multi-GeV energies, this is particularly apparent for tensor interactions at energies ≳ 6GeV

Noemi Rocco, nrocco@fnal.gov
Fermilab

Using Bayesian ANN for electron-nucleus scattering

J. Sobczyk, NR, A. Lovato, arxiv:2406.06292

The inclusive electron-nucleus cross section can be written in terms of the longitudinal and transverse response function

$$\left(\frac{d^2\sigma}{dE'd\Omega'}\right)_e = \left(\frac{d\sigma}{d\Omega'}\right)_{\rm M}\left[\frac{q^4}{\mathbf{q}^4}R_L(\mathbf{q},\omega) + \left(\tan^2\frac{\theta}{2} - \frac{1}{2}\frac{q^2}{\mathbf{q}^2}\right)R_T(\mathbf{q},\omega)\right]$$

Traditionally, the **Rosenbluth separation** is adopted to obtain $R_L(\mathbf{q},\omega)$ and $R_T(\mathbf{q},\omega)$

$$\Sigma(\mathbf{q},\omega,\epsilon) = \epsilon\,\frac{\mathbf{q}^4}{Q^4}\left(\frac{d^2\sigma}{dE'd\Omega'}\right)_e \Bigg/ \left(\frac{d\sigma}{d\Omega'}\right)_{\rm M} = \epsilon R_L(\mathbf{q},\omega) + \frac{1}{2}\frac{\mathbf{q}^2}{Q^2}R_T(\mathbf{q},\omega)$$

Photon polarization

As θ ranges between 180 to 0 degrees, ϵ varies between 0 and 1. Within this approach, R_L is the **slope** while $(\mathbf{q}^2/2Q^2)R_T$ is the **intercept** of the linear fit to data

Noemi Rocco, nrocco@fnal.gov

Using Bayesian ANN for electron-nucleus scattering

We used ANN architecture to obtain the **longitudinal** and **transverse responses**

- We built **two completely independent nets** proving the longitudinal and transverse responses.

We train our ANN using the quasielastic electron nucleus scattering archive of arXiv:nucl-ex/0603032 considering five different light and medium-mass nuclei, symmetric: ^{4}He, ^{6}Li, ^{12}C, ^{16}O and ^{40}Ca.

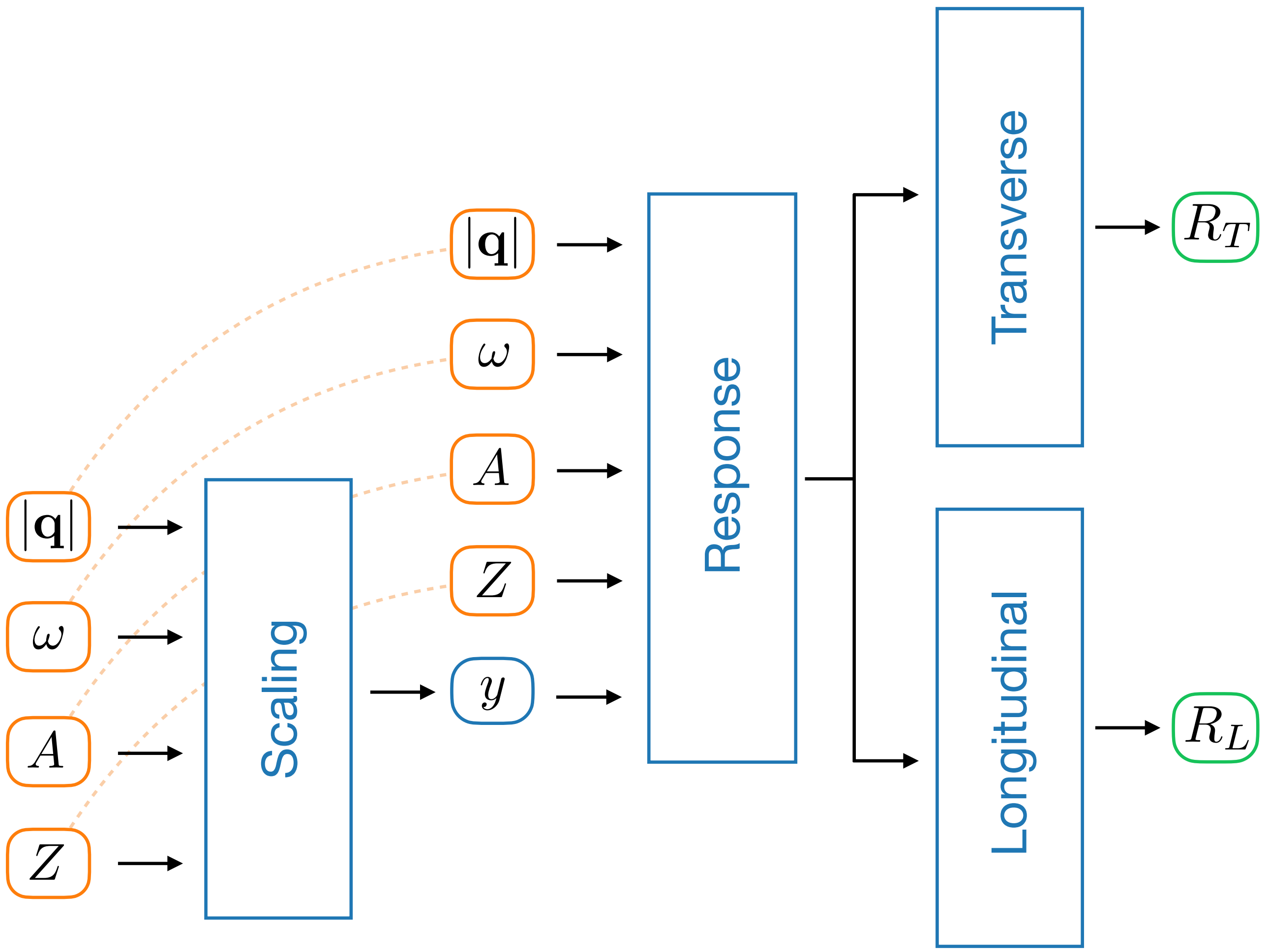

We used **Bayesian statistics** to quantify the uncertainty of the ANN: treat the weights $\mathscr{W}$ as a probability distribution. The posterior distribution of $\mathscr{W}$ is sampled using the **NumPyro No-U-Turn Sampler** extension of HMC. We also implemented the standard HMC algorithm and validated results.

Noemi Rocco, nrocco@fnal.gov
Fermilab

Using Bayesian ANN for electron-nucleus scattering

Results: Cross sections for different nuclei

J. Sobczyk, NR, A. Lovato, arxiv:2406.06292

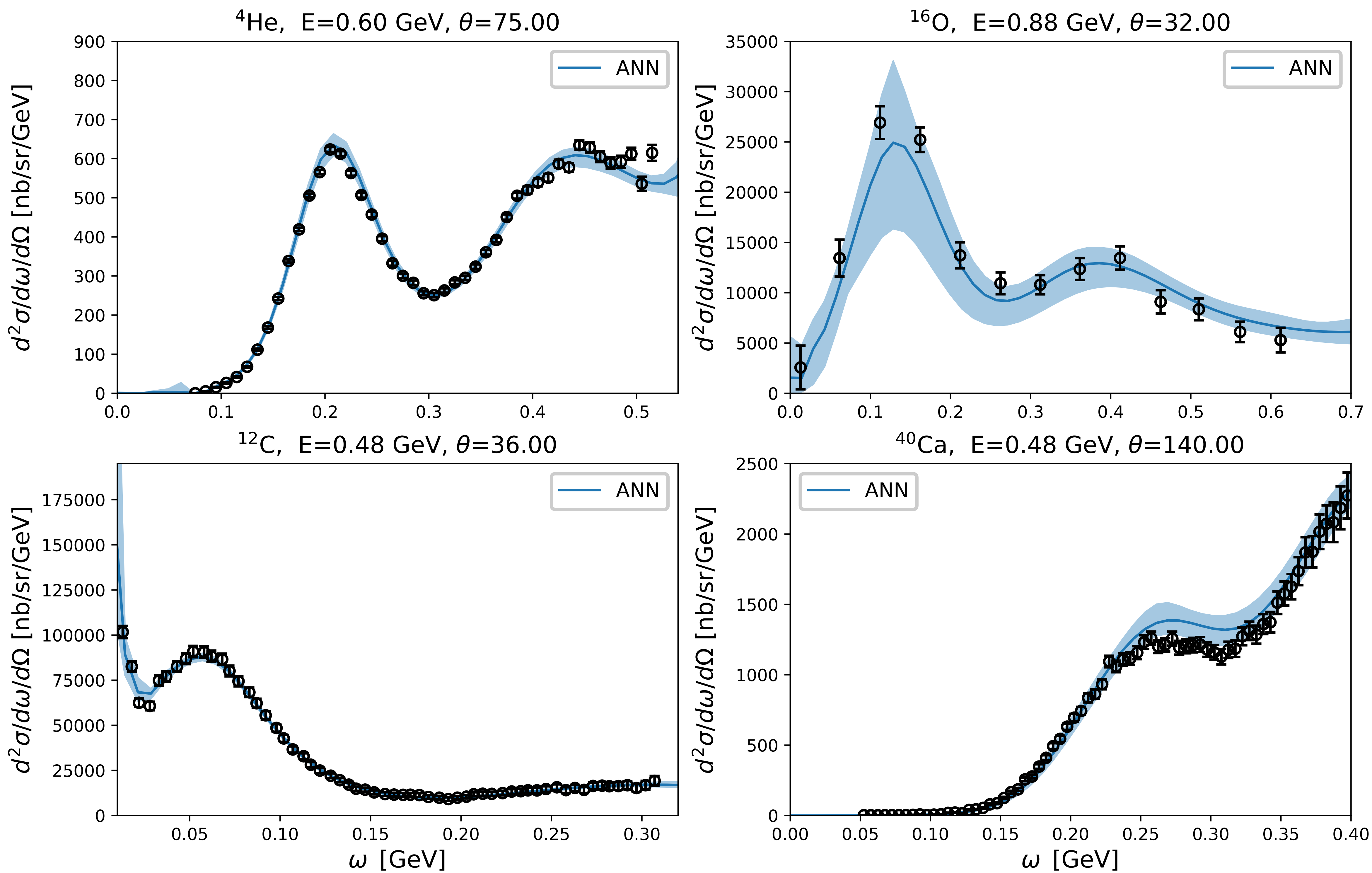

Noemi Rocco, nrocco@fnal.gov

Using Bayesian ANN for electron-nucleus scattering

J. Sobczyk, NR, A. Lovato, arxiv:2406.06292

Results: Electromagnetic responses

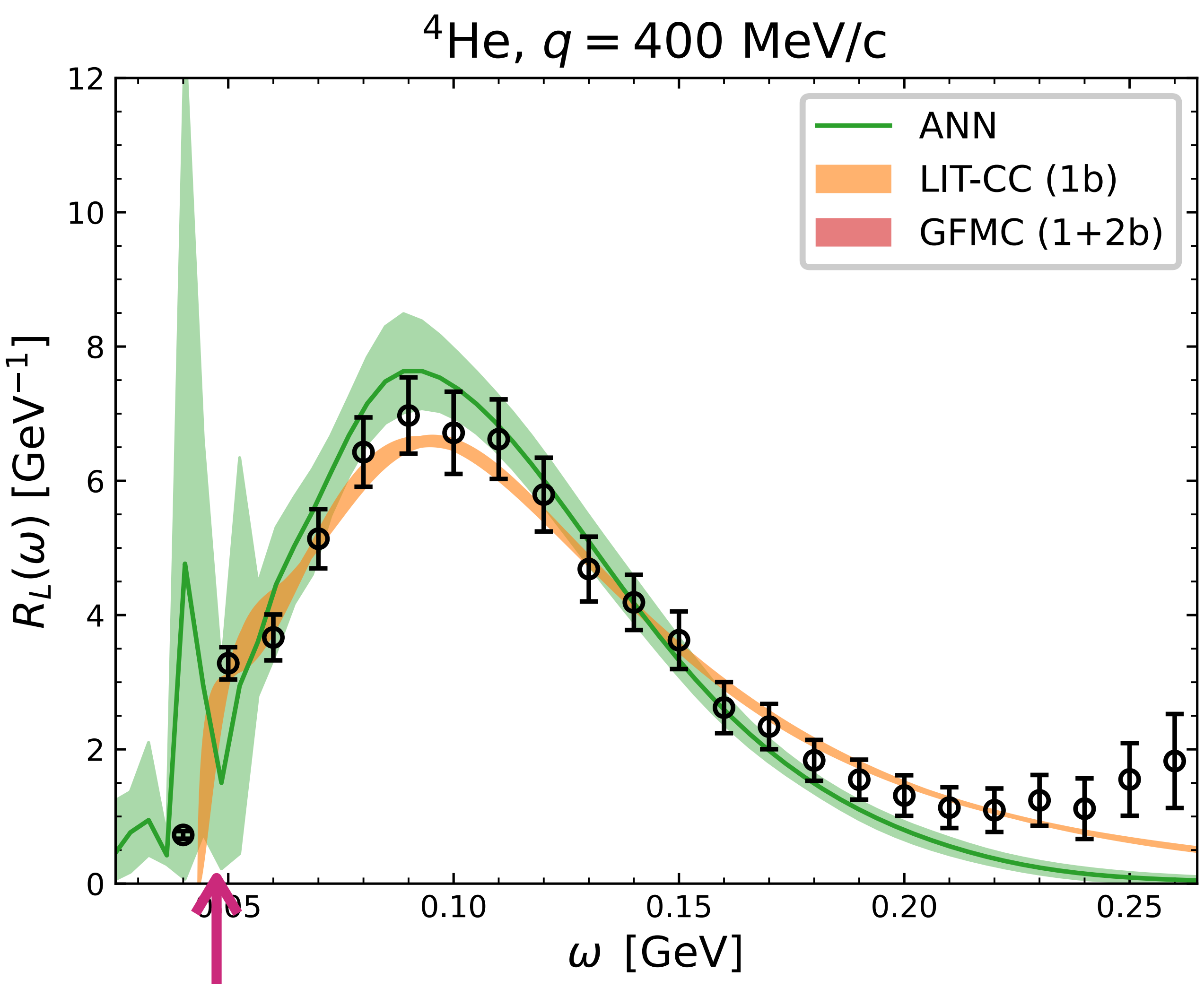

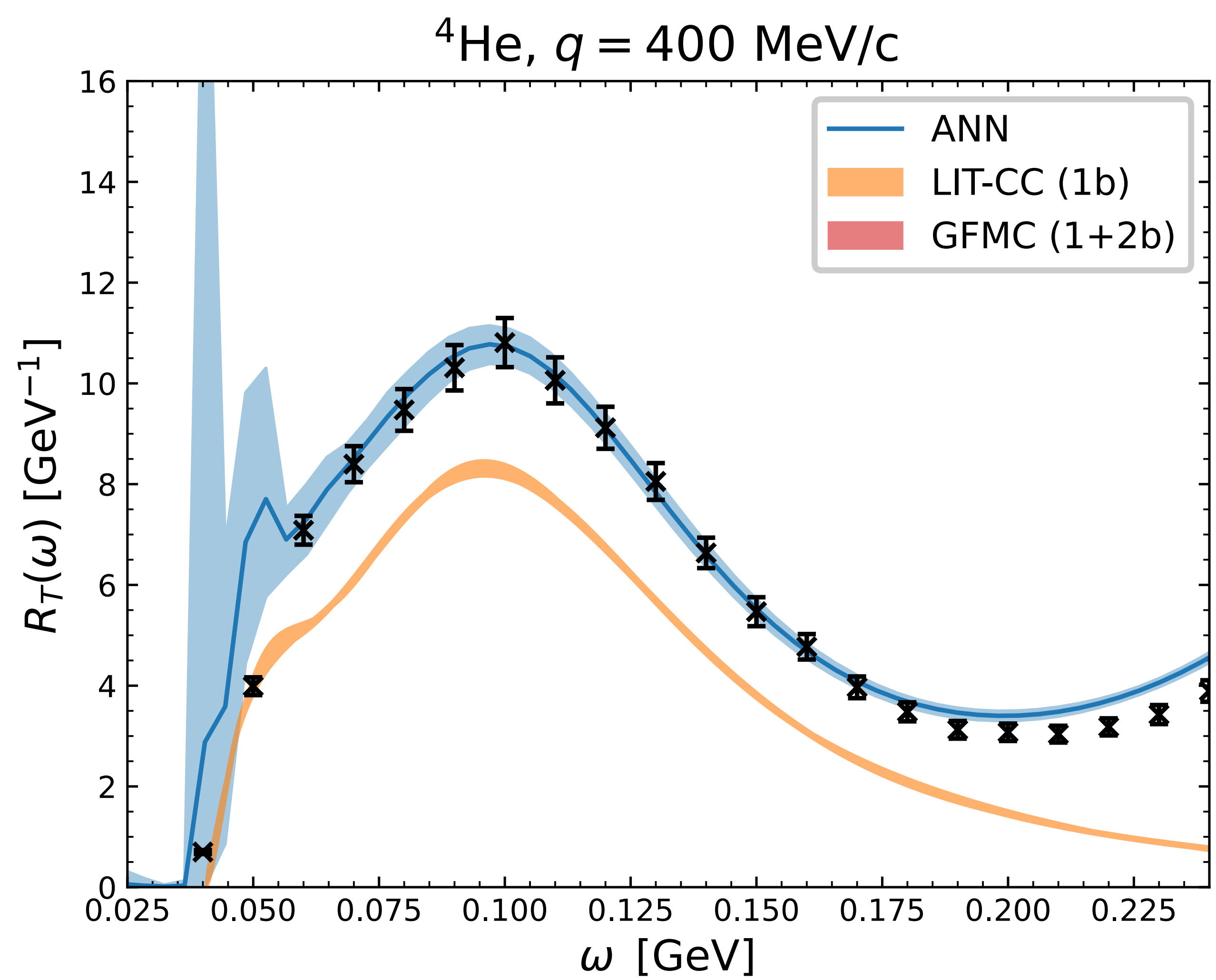

Low lying nuclear states

Contributions from elastic and low-lying inelastic transitions are explicitly removed from the GFMC responses and the Rosenbluth analysis, while they are present in the ANN curves

Noemi Rocco, nrocco@fnal.gov

Using Bayesian ANN for electron-nucleus scattering

J. Sobczyk, NR, A. Lovato, arxiv:2406.06292

Results: Electromagnetic responses

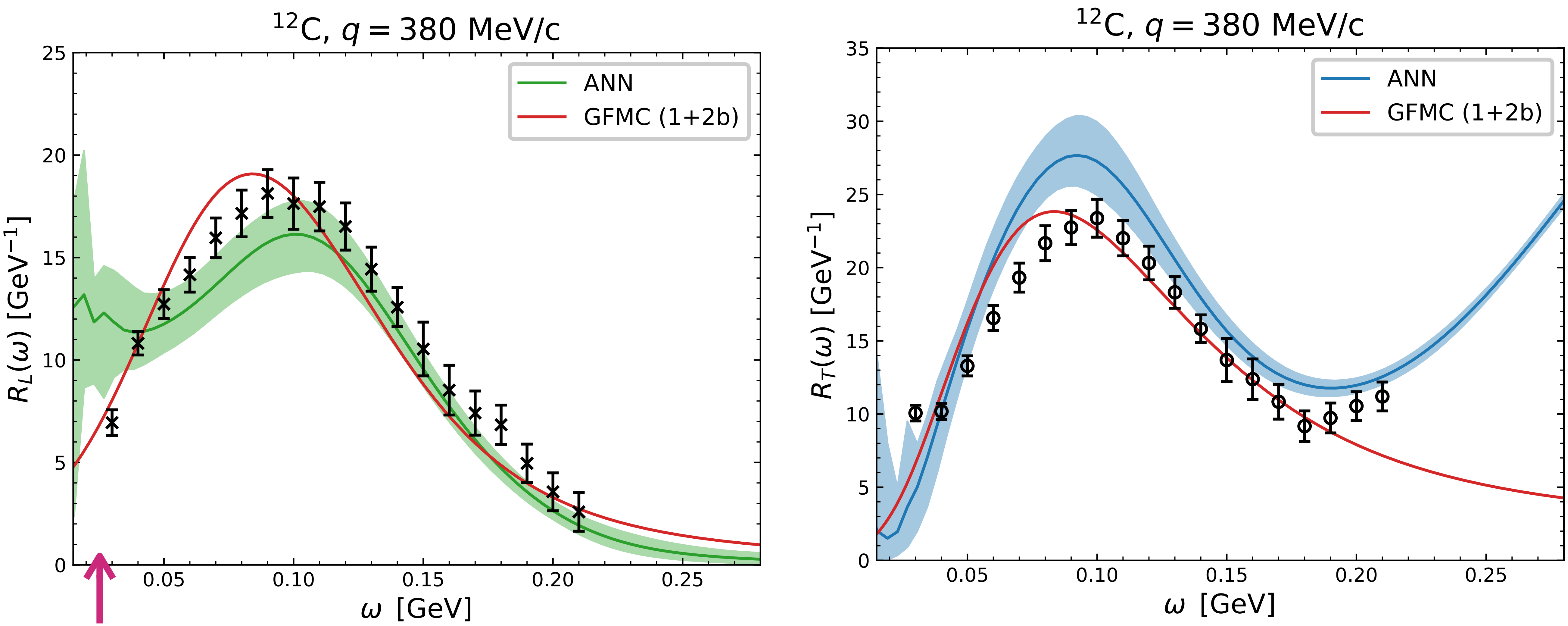

Low lying nuclear states

Contributions from elastic and low-lying inelastic transitions are explicitly removed from the GFMC responses and the Rosenbluth analysis, while they are present in the ANN curves

Noemi Rocco, nrocco@fnal.gov
Fermilab

Using Bayesian ANN for electron-nucleus scattering

J. Sobczyk, NR, A. Lovato, arxiv:2406.06292

Results: Electromagnetic responses

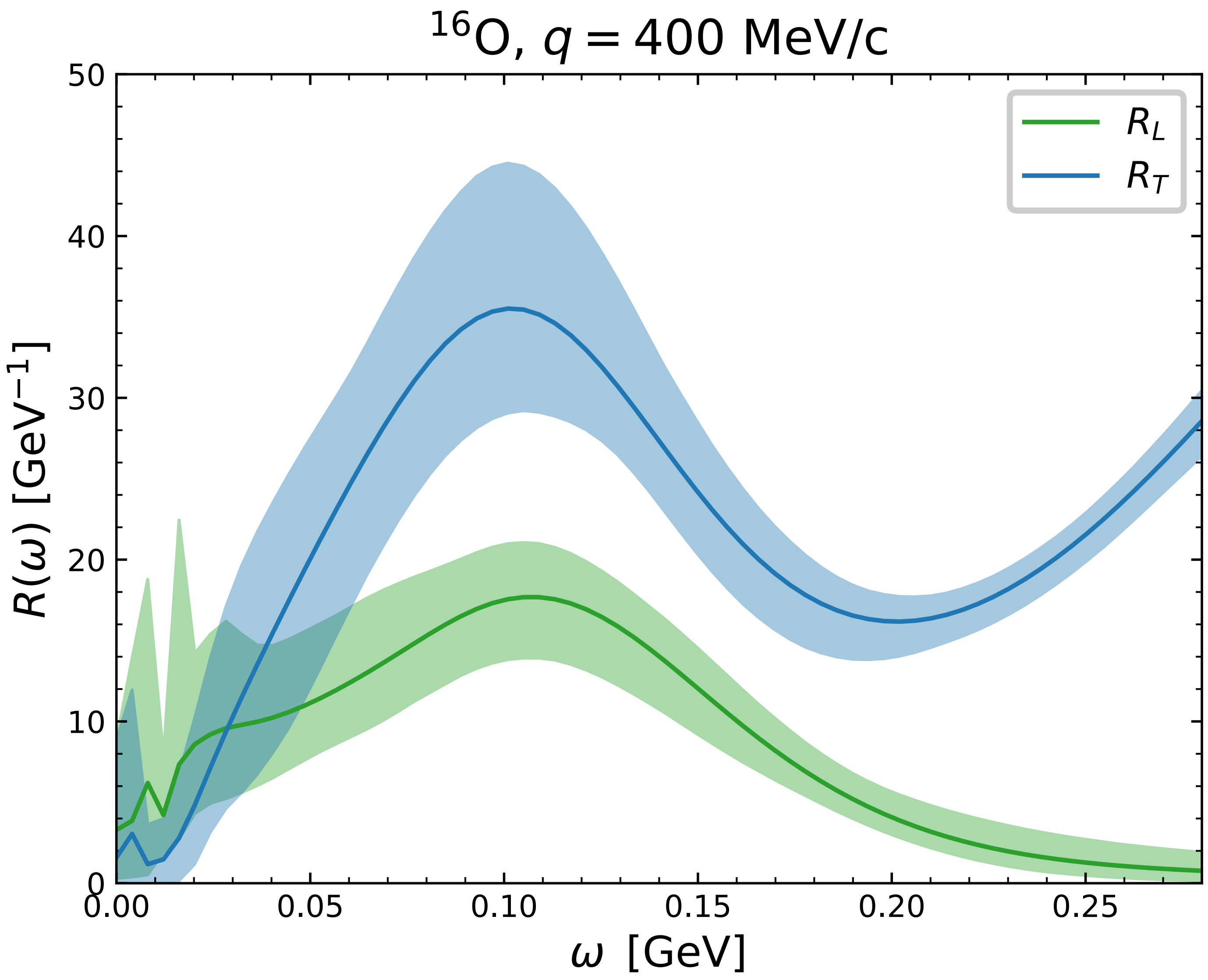

First separation of the longitudinal and transverse responses of ^{16}O. Large uncertainty bands reflect the **scarcity of inclusive cross section data.**

Noemi Rocco, nrocco@fnal.gov

Using Bayesian ANN for electron-nucleus scattering

J. Sobczyk, NR, A. Lovato, arxiv:2406.06292

Results: Electromagnetic responses

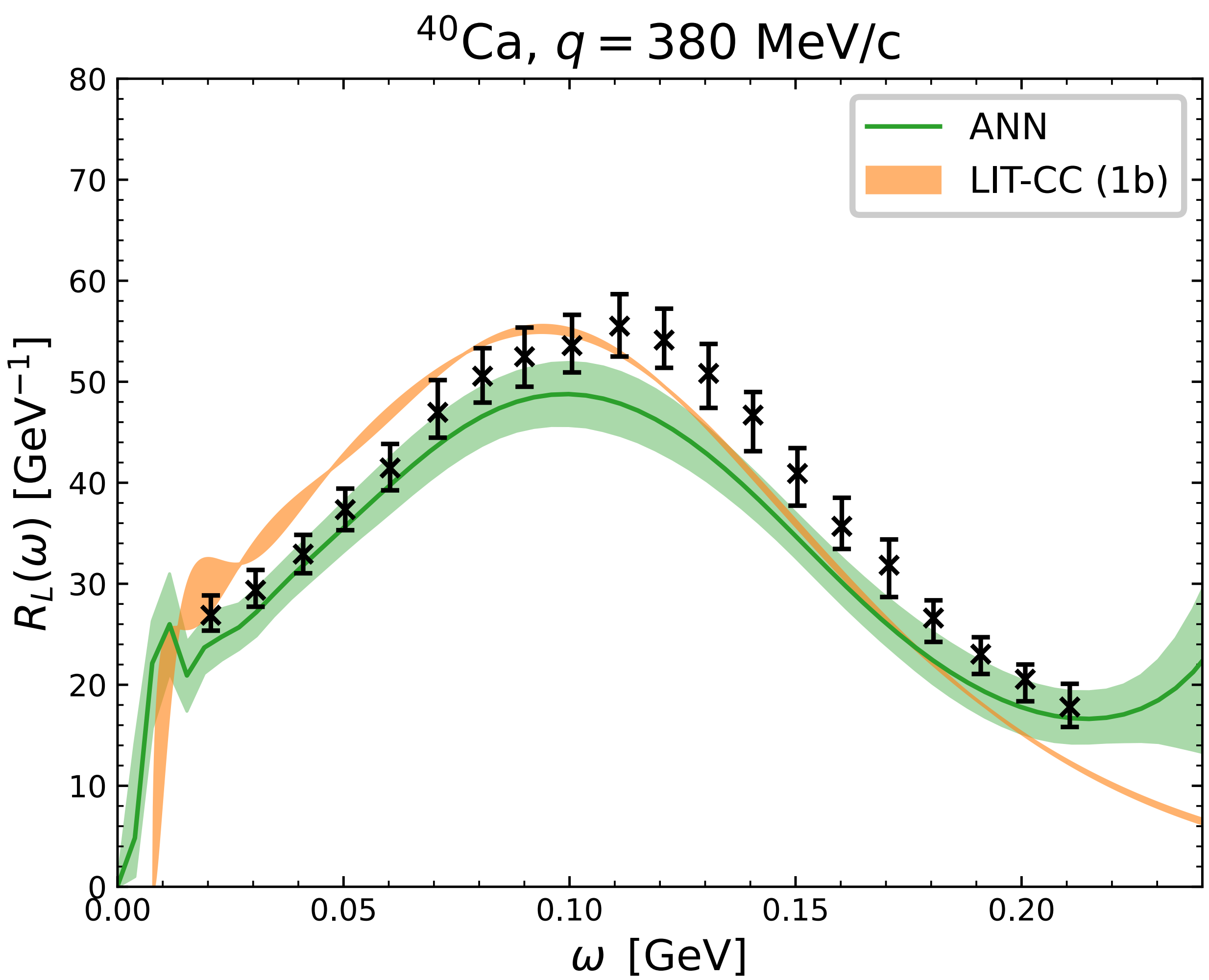

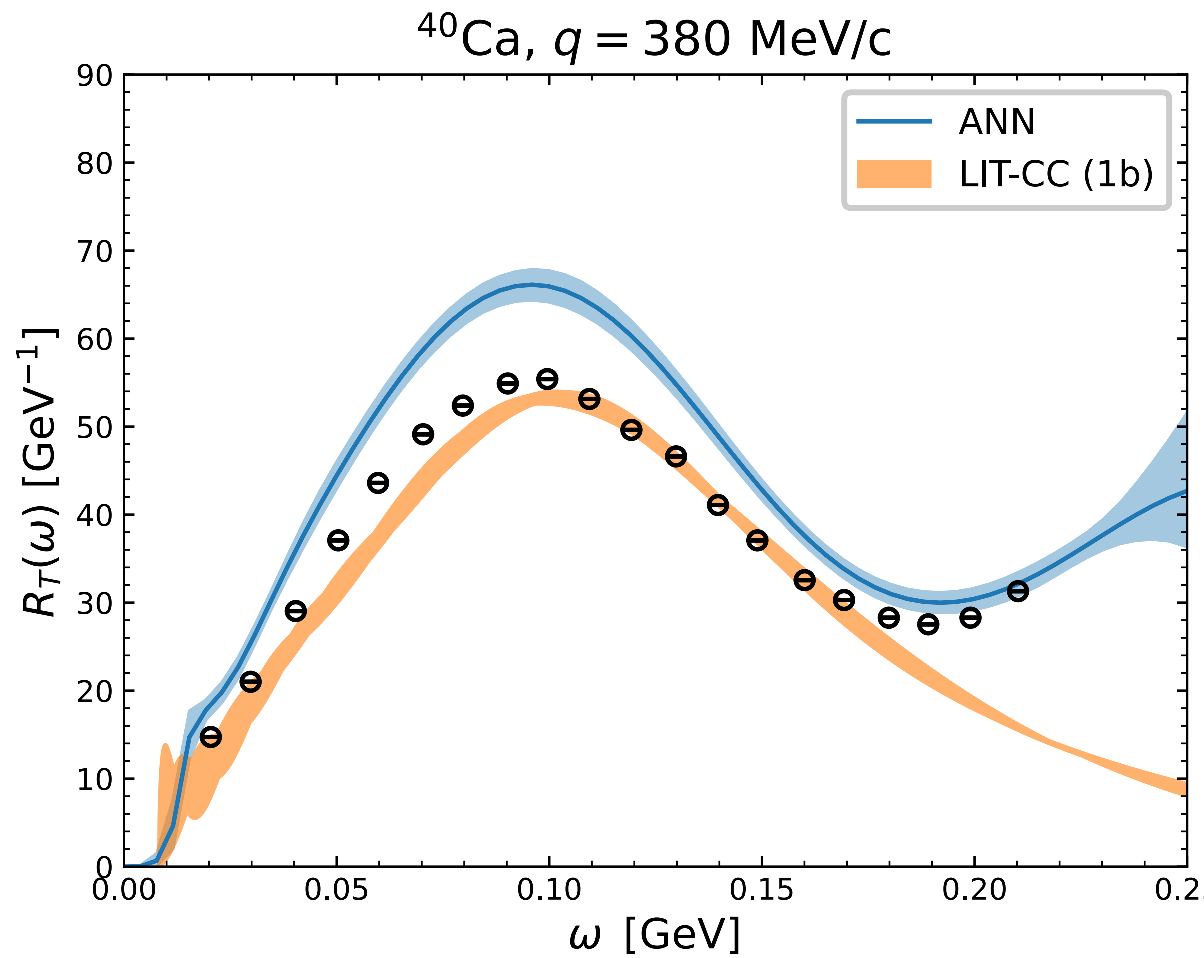

Note increasing error bars for large ω reflecting the scarcity of data for 40Ca in the high energy-momentum region. The net is learning from other nuclei in this region.

Dedicated discussion on the Rosenbluth separation carried out using two different experiments.

Noemi Rocco, nrocco@fnal.gov

Conclusions

- Neutrino oscillation experiments are entering a new precision era

- To match these precision goals accurate predictions of neutrino cross sections are crucial

  Ab initio methods: almost exact results but limited in energy, fully inclusive

  Approaches based on factorization schemes are being further developed

- Uncertainty associated with the theory prediction of the hard interaction vertex needs to be assessed. Initial work has been carried out in this direction studying the dependence on:

  Form factors: one- and two-body currents, resonance/π production

  Error of factorizing the hard interaction vertex / using a non relativistic approach

- Combine state-of-the art neutrino-nucleus calculations with BSM theories is gaining momentum; UQ is very interesting (and challenging) in this case as well

Noemi Rocco, nrocco@fnal.gov

Thank you for your attention!

Including the one- and two-body interference

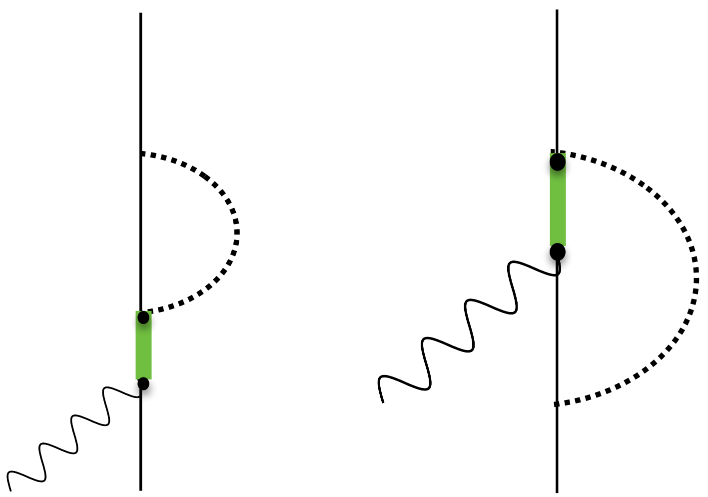

We recently included interference effects between one- and two-body currents yielding single nucleon knock-out

Observe a small quenching in the longitudinal channel and an enhancement in the q.e. peak in the transverse → agreement with the GFMC

N. Steinberg, NR, A. Lovato, arXiv: 2312.12545

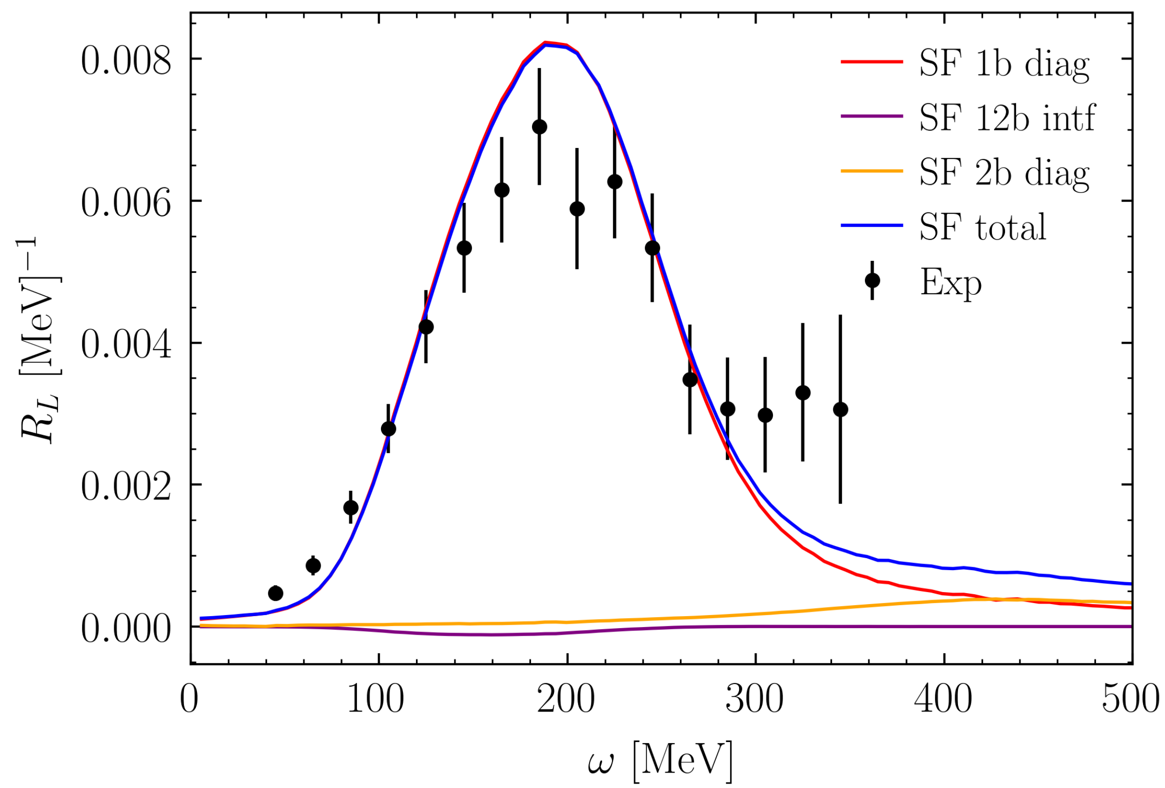

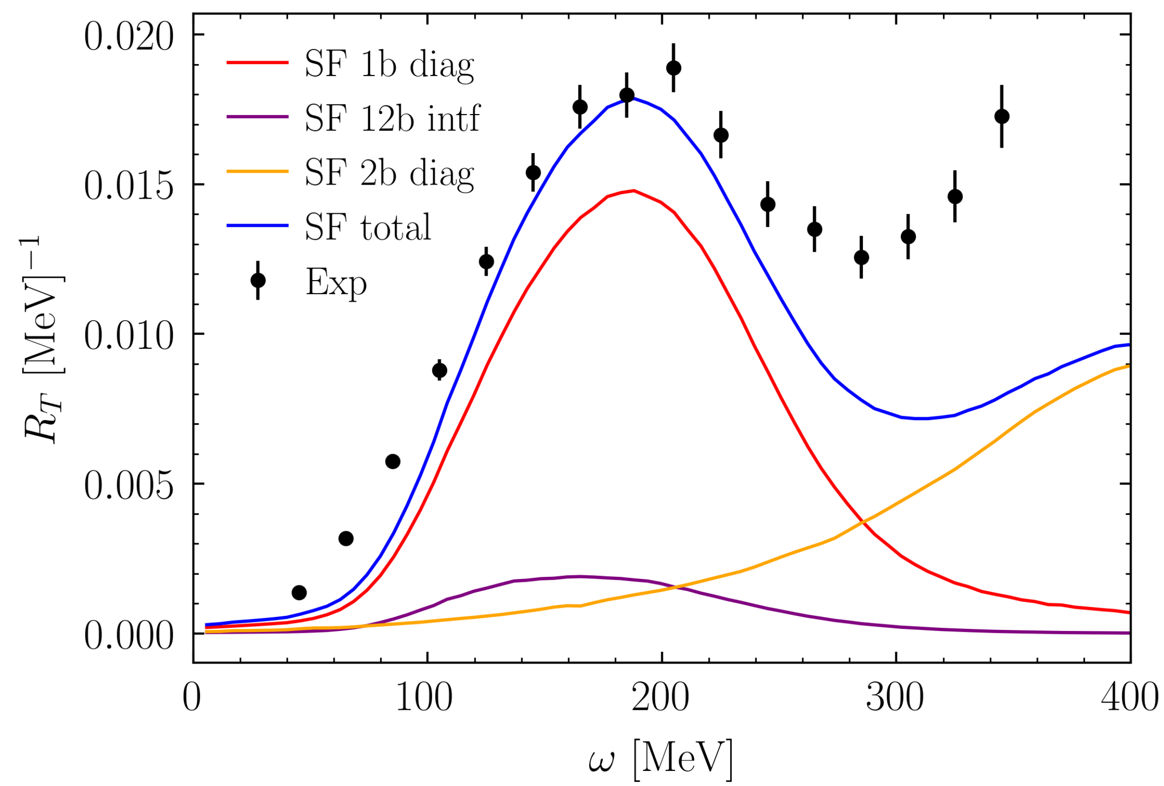

Noemi Rocco, nrocco@fnal.gov

Form factors - hadronic m.e.

Z. Tabrizi, J. Kopp, NR, arxiv: 2401.07902

$$\langle p(p_p)|\bar{q}_u q_d|n(p_n)\rangle = G_S(Q^2)\,\bar{u}_p(p_p)u_n(p_n)\,,$$

$$\langle p(p_p)|\bar{q}_u \gamma_5 q_d|n(p_n)\rangle = G_P(Q^2)\,\bar{u}_p(p_p)\gamma_5 u_n(p_n)\,,$$

$$\langle p(p_p)|\bar{q}_u \sigma_{\mu\nu} q_d|n(p_n)\rangle = \bar{u}_p(p_p)\Big[G_T(Q^2)\sigma_{\mu\nu} - \frac{i}{M_N}G_T^{(1)}(Q^2)(q_\mu\gamma_\nu - q_\nu\gamma_\mu) - \frac{i}{M_N^2}G_T^{(2)}(Q^2)(q_\mu P_\nu - q_\nu P_\mu) - \frac{i}{M_N}G_T^{(3)}(Q^2)(\gamma_\mu \not{q}\gamma_\nu - \gamma_\nu \not{q}\gamma_\mu)\Big]u_n(p_n)$$

Noemi Rocco, nrocco@fnal.gov

Form factors - new interactions

Z. Tabrizi, J. Kopp, NR, arxiv: 2401.07902

- Induced pseudo-scalar (pion-pole dominance)

$$\tilde{G}_P(Q^2) = -\frac{4M_N^2}{Q^2 + m_\pi^2} G_A(Q^2) \,.$$

- Induced scalar we used a constituent quark model parametrization

$$\tilde{G}_S(Q^2) = \frac{2M_N}{(m_u + m_d)^{\mathrm{CQM}}} \left(\frac{\delta M_N^{QCD}}{2M_N} g_A - \frac{\delta m_q}{(m_u + m_d)^{\mathrm{CQM}}} \right) G_V(Q^2) \,,$$

- Tensor current. We adopt the isospin symmetric limit:

$$\begin{aligned} \langle p(p_p) | \bar{u}\sigma^{\mu\nu} d | n(p_n) \rangle &= \langle p(p_p) | \bar{u}\sigma^{\mu\nu} u - \bar{d}\sigma^{\mu\nu} d | p(p_p) \rangle \\ &= \langle n(p_n) | \bar{d}\sigma^{\mu\nu} d - \bar{u}\sigma^{\mu\nu} u | n(p_n) \rangle \,. \end{aligned}$$

$$\begin{aligned} G_T(Q^2) &= F_{1,T}^u(Q^2) - F_{1,T}^d(Q^2) \,, \\ G_T^{(1)}(Q^2) &= F_{2,T}^u(Q^2) - F_{2,T}^d(Q^2) \,, \\ G_T^{(2)}(Q^2) &= F_{3,T}^u(Q^2) - F_{3,T}^d(Q^2) \,, \end{aligned}$$

- *M. Hoferichter et al, Phys.Rev.Lett. 124, 199901 (2020)*

Using Bayesian ANN for electron-nucleus scattering

We used **Bayesian statistics** to quantify the uncertainty of the ANN. We treat the weights $\mathscr{W}$ as a probability distribution.

The posterior probability of the parameters $\mathscr{W}$ given the measured cross sections Y can be written as

$$P(\mathscr{W}\,|\,Y) = \frac{P(Y\,|\,\mathscr{W})P(\mathscr{W})}{P(Y)}$$

We assign a normal Gaussian prior for each neural network parameter and assume a **Gaussian distribution for the likelihood** based on a loss function obtained from a **least-squares** fit to the empirical data

$$P(Y\,|\,\mathscr{W}) = \exp\left(-\frac{\chi^2}{2}\right) \qquad \chi^2 = \sum_{i=1}^{N} \frac{\left[y_i - \hat{y}_i(\mathscr{W}))\right]^2}{\sigma_i^2}$$

We increase the experimental errors σ_i listed in arXiv:nucl-ex/0603032 including an additional term proportional to the experimental cross section value: $\sigma_i \rightarrow \sigma_i + 0.05 y_i$.

The posterior distribution is sampled using the **NumPyro No-U-Turn Sampler** extension of HMC. We also implemented the standard HMC algorithm and validated results.

Noemi Rocco, nrocco@fnal.gov

Using Bayesian ANN for electron-nucleus scattering

J. Sobczyk, NR, A. Lovato, arxiv:2406.06292

Results: Electromagnetic responses

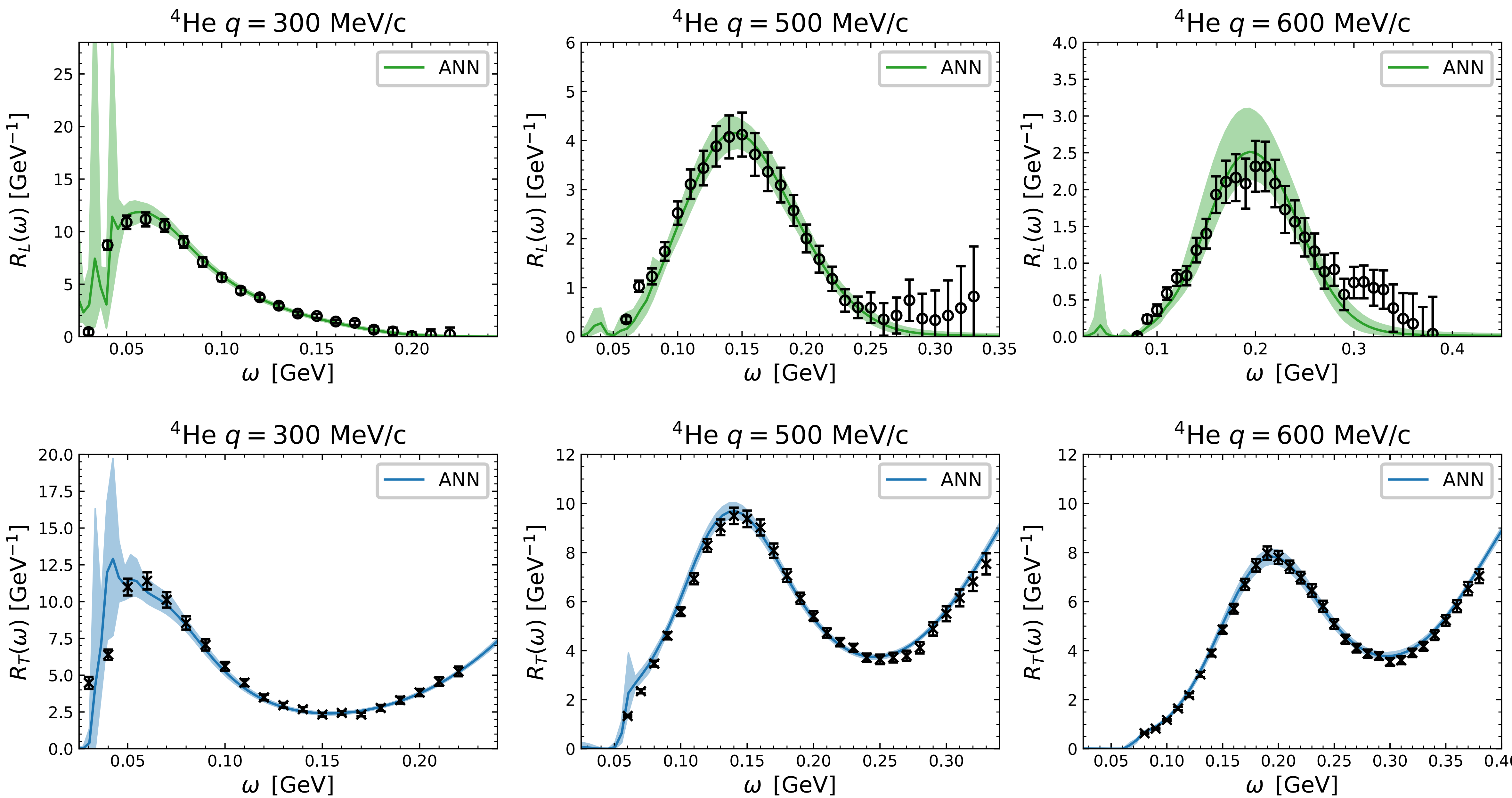

Using Bayesian ANN for electron-nucleus scattering

J. Sobczyk, NR, A. Lovato, arxiv:2406.06292

Results: Electromagnetic responses

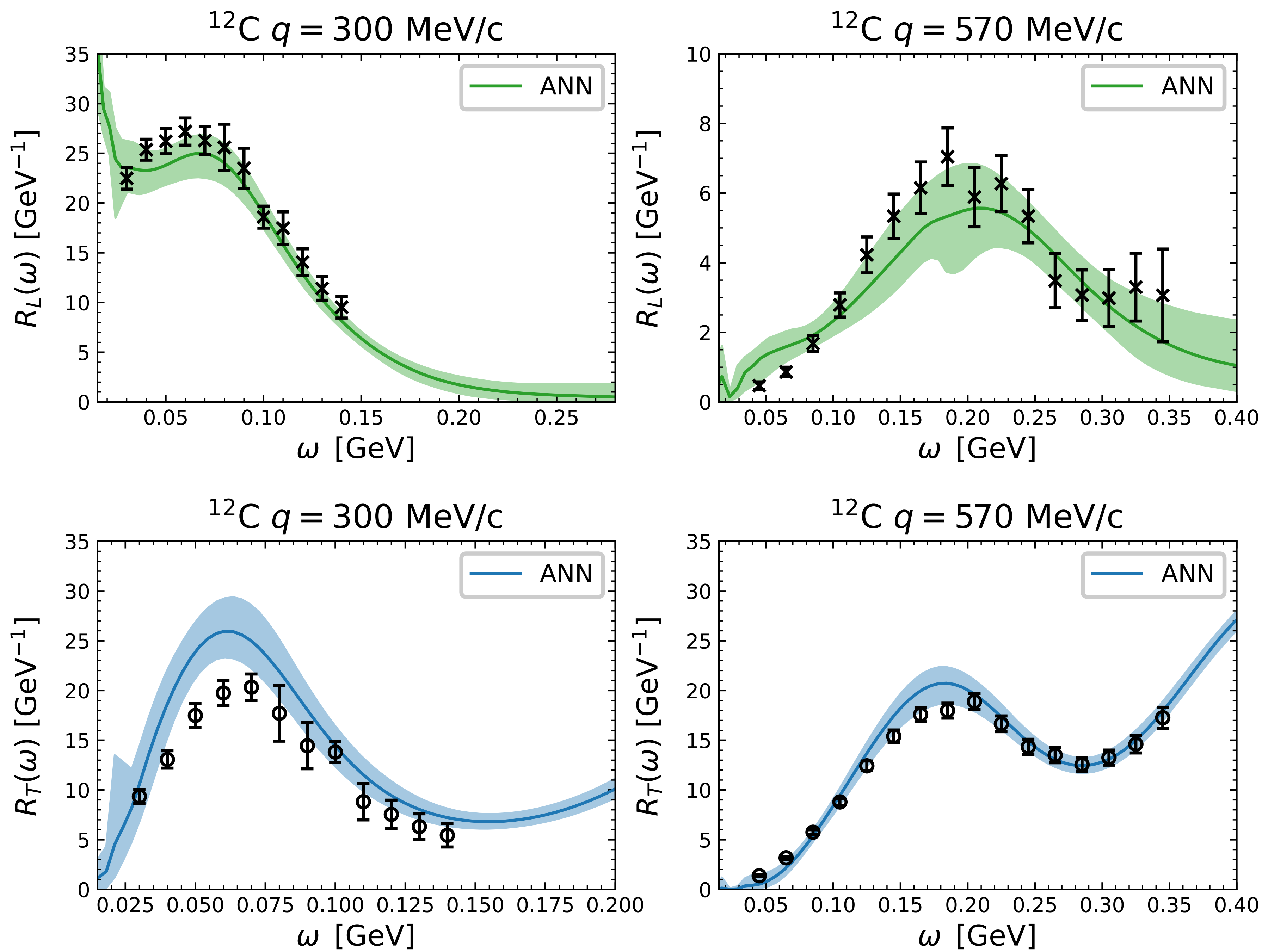

Noemi Rocco, nrocco@fnal.gov

Using Bayesian ANN for electron-nucleus scattering

J. Sobczyk, NR, A. Lovato, arxiv:2406.06292

Results: Electromagnetic responses

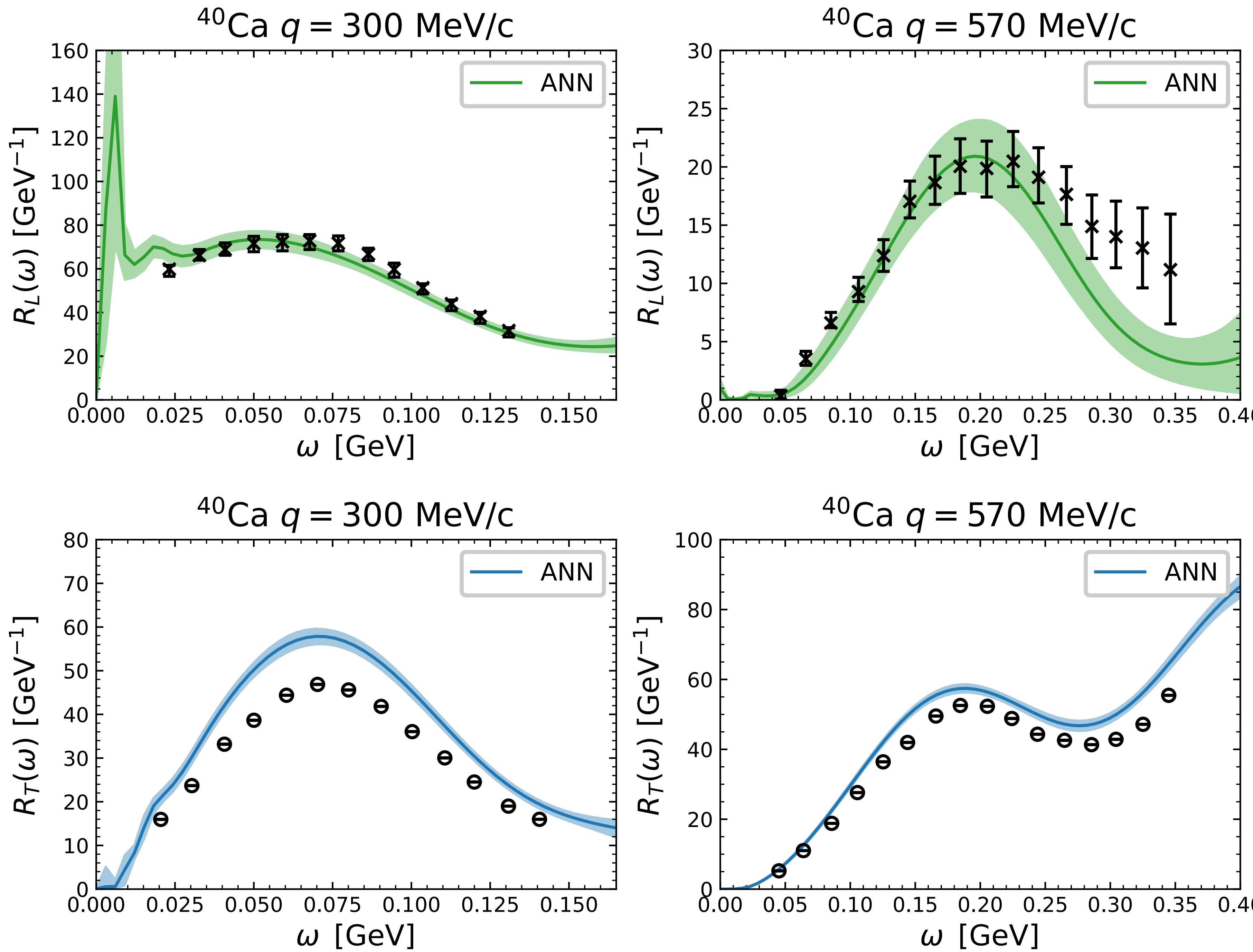

Noemi Rocco, nrocco@fnal.gov

Using Bayesian ANN for electron-nucleus scattering

J. Sobczyk, NR, A. Lovato, arxiv:2406.06292

Results: Electromagnetic responses

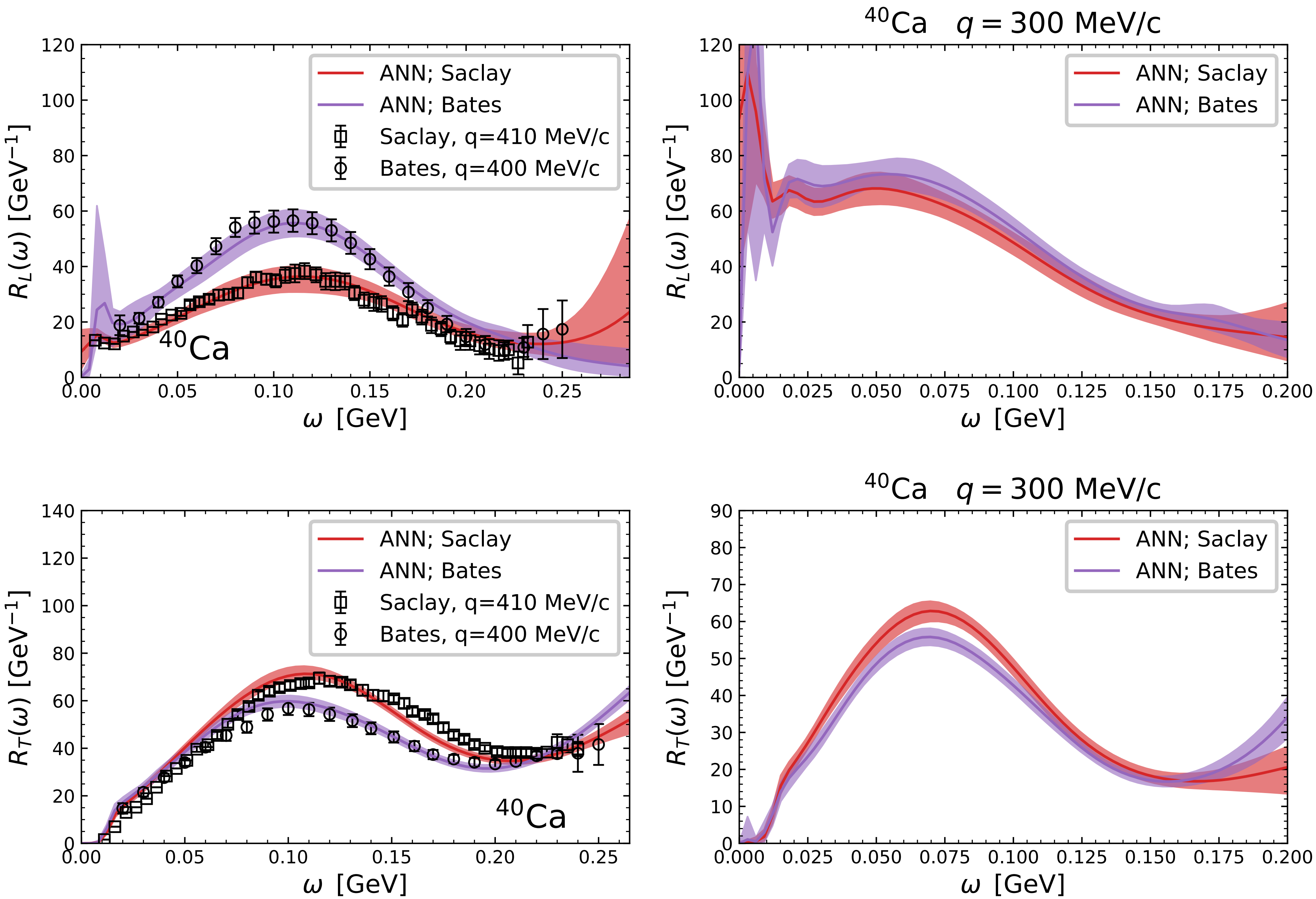

Noemi Rocco, nrocco@fnal.gov
Fermilab

Delta contribution to MEC

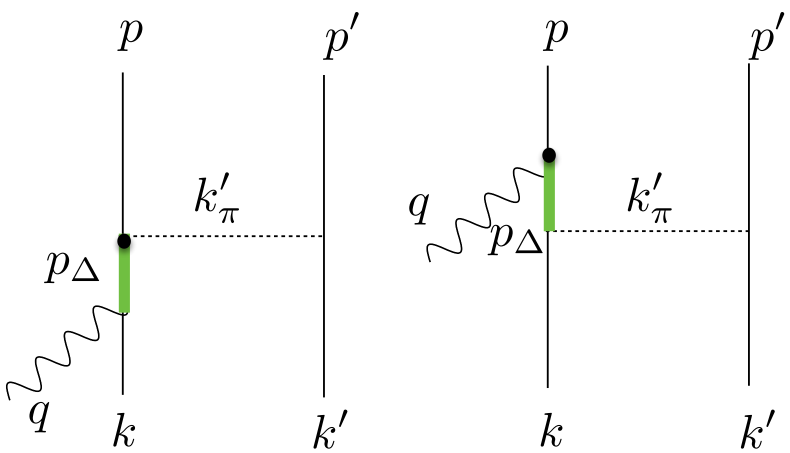

Diagrams including the Delta current depend on many parameters.

$$(j_a^\mu)_A = (k'_\pi)^\alpha G_{\alpha\beta}(p_\Delta)\Big[\frac{C_3^A}{m_N}\left(g^{\beta\mu}\not{q} - q^\beta\gamma^\mu\right) + \frac{C_4^A}{m_N^2}\left(g^{\beta\mu} q\cdot p_\Delta - q^\beta p_\Delta^\mu\right) + C_5^A g^{\beta\mu} + \frac{C_6^A}{m_N^2} q^\mu q^\alpha\Big],$$

Parametrization chosen for the vector ff:

$$C_5^A = \frac{1.2}{(1-q^2/M_{A\Delta})^2} \times \frac{1}{1-q^2/(3M_{A\Delta})^2)},$$

Current extractions of C_A^5 (0) rely on single pion production data from deuterium bubble chamber experiments; estimated uncertainty ~ 15 %

Delta decay width:

$$\Gamma(p_\Delta) = \frac{(4f_{\pi N\Delta})^2}{12\pi m_\pi^2}\frac{|\mathbf{d}|^3}{\sqrt{s}}(m_N + E_d)R(\mathbf{r}^2) \qquad R(\mathbf{r}^2) = \left(\frac{\Lambda_R^2}{\Lambda_R^2 - \mathbf{r}^2}\right)$$

Noemi Rocco, nrocco@fnal.gov

ACHILLES: A CHicago Land Lepton Event Simulator

The propagation of **nucleons** through the **<u>nuclear medium</u>** is crucial in the analysis of electron-nucleus scattering and neutrino oscillation experiments.

- Elastic scattering
- Charge exchange
- Pion Production
- Absorption
- ….

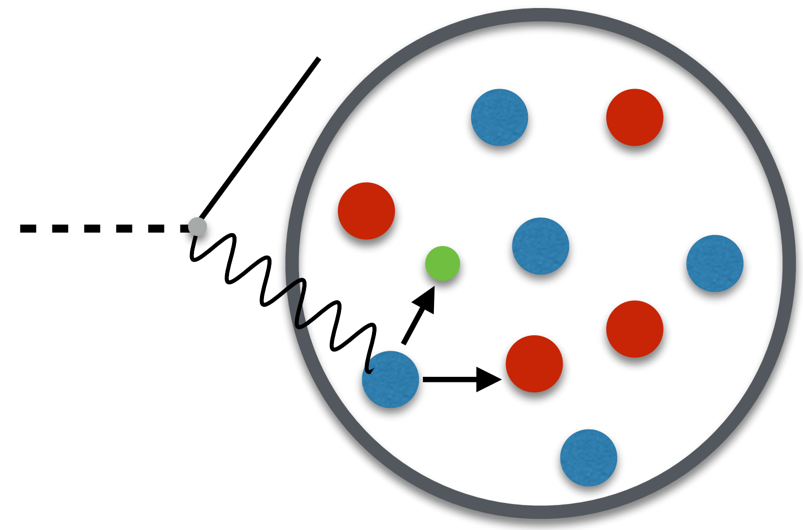

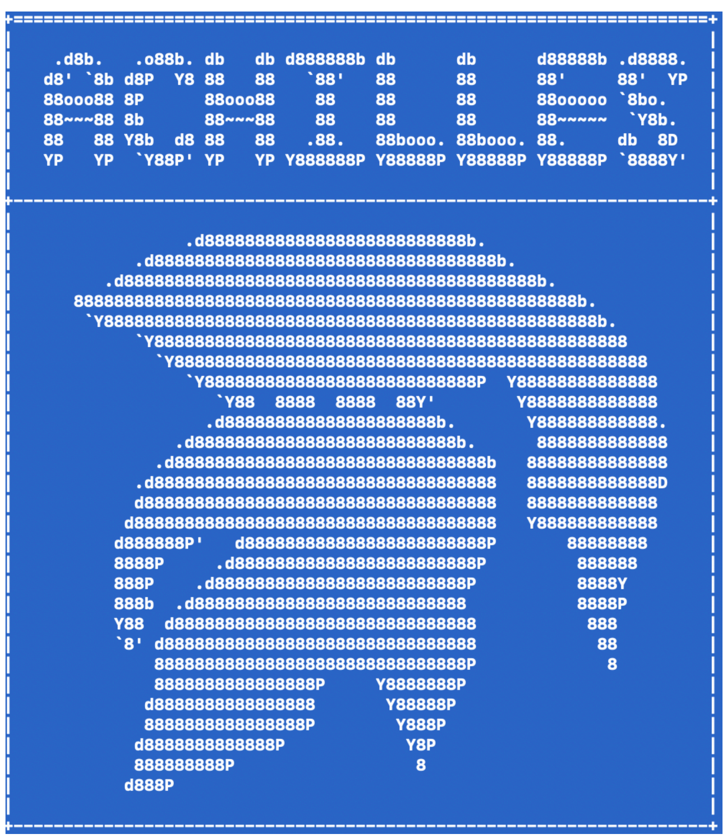

- Develop a theory driven, modular event generator
- Provide automated BSM calculations for neutrino experiments
- Uses realistic QMC nuclear calculations as inputs

J.Isaacson, W Jay, A. Lovato, P Machado, NR:

- *arXiv:2205.06378*
- *PRD 105 (2022) 9, 096006*
- *PRC 103 (2021) 1, 015502*

Fermilab

Noemi Rocco, nrocco@fnal.gov

ACHILLES: A CHicago Land Lepton Event Simulator

Completed the implementation of QE, 12b interference and pion production for both electron and neutrino sectors.

BSM scenarios can be readily implemented (in the leptonic sector), using the available reaction mechanisms. Next studies: dark neutrinos, HNL produced via magnetic moments

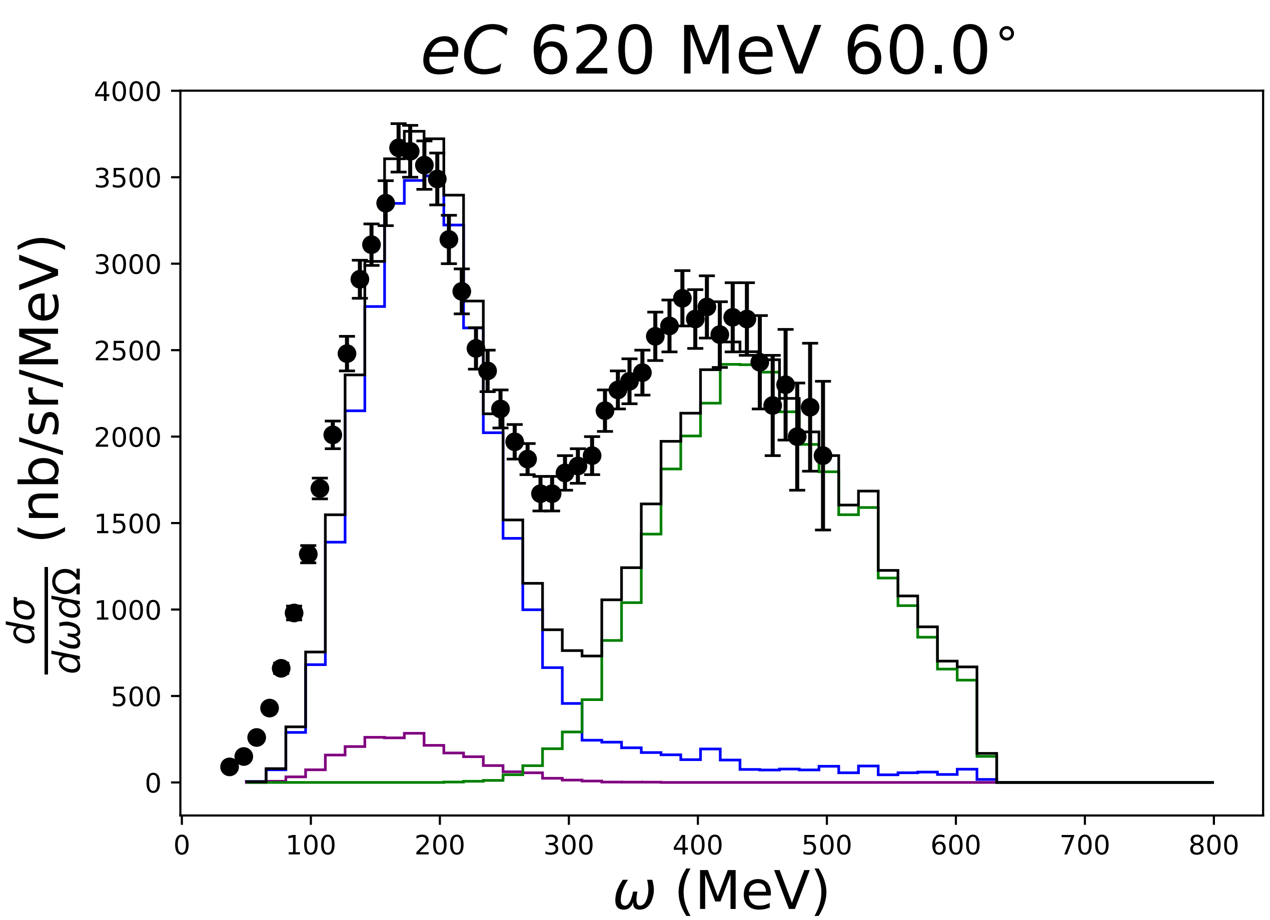

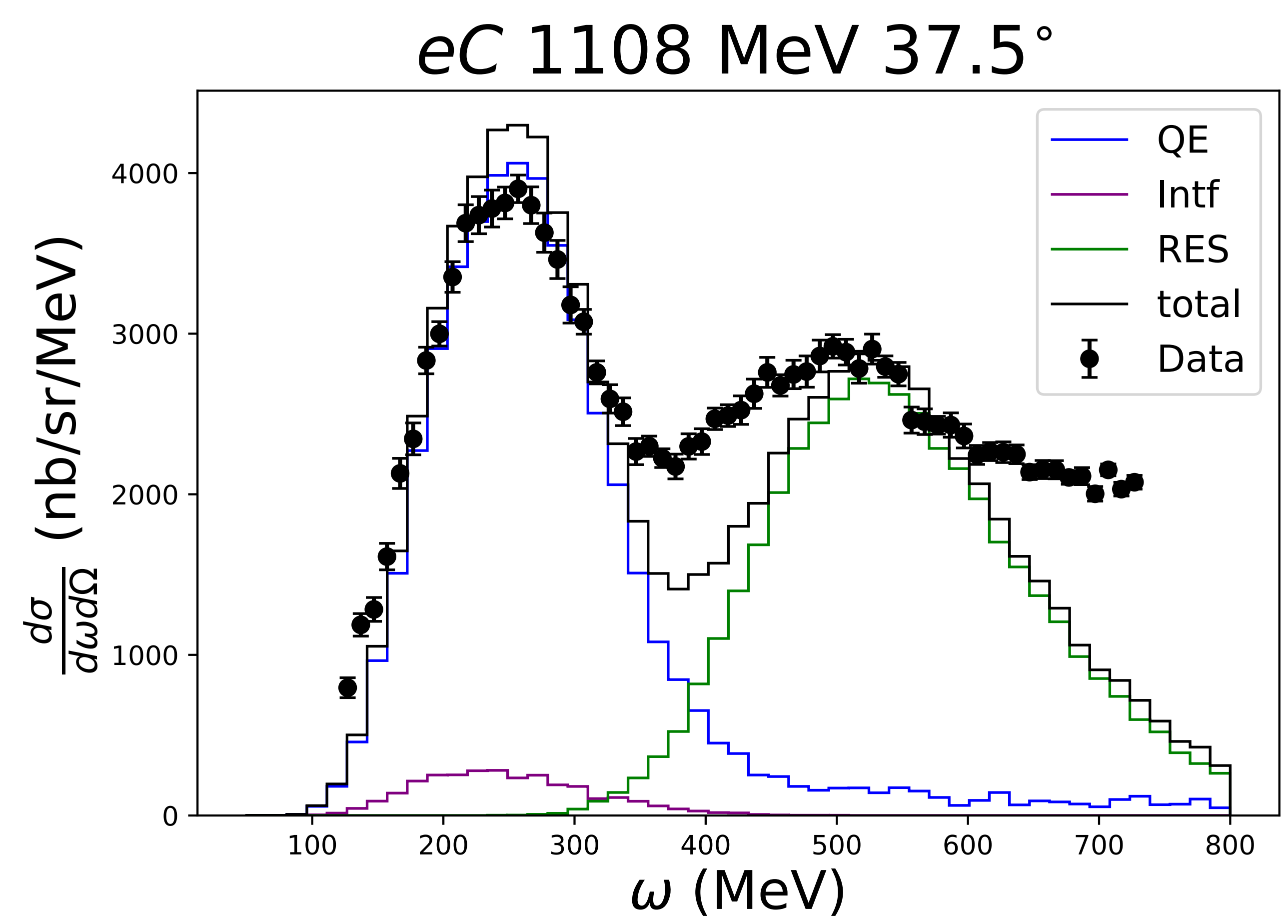

N. Steinberg, J. Isaacson, NR, et al, in preparation

Noemi Rocco, nrocco@fnal.gov

QMC Spectral function of light nuclei

- Single-nucleon spectral function:

$$P_{p,n}(\mathbf{k}, E) = \sum_n \left| \langle \Psi_0^A | [|k\rangle |\Psi_n^{A-1}\rangle] \right|^2 \times \delta(E + E_0^A - E_n^{A-1}) = P^{MF}(\mathbf{k}, E) + P^{corr}(\mathbf{k}, E)$$

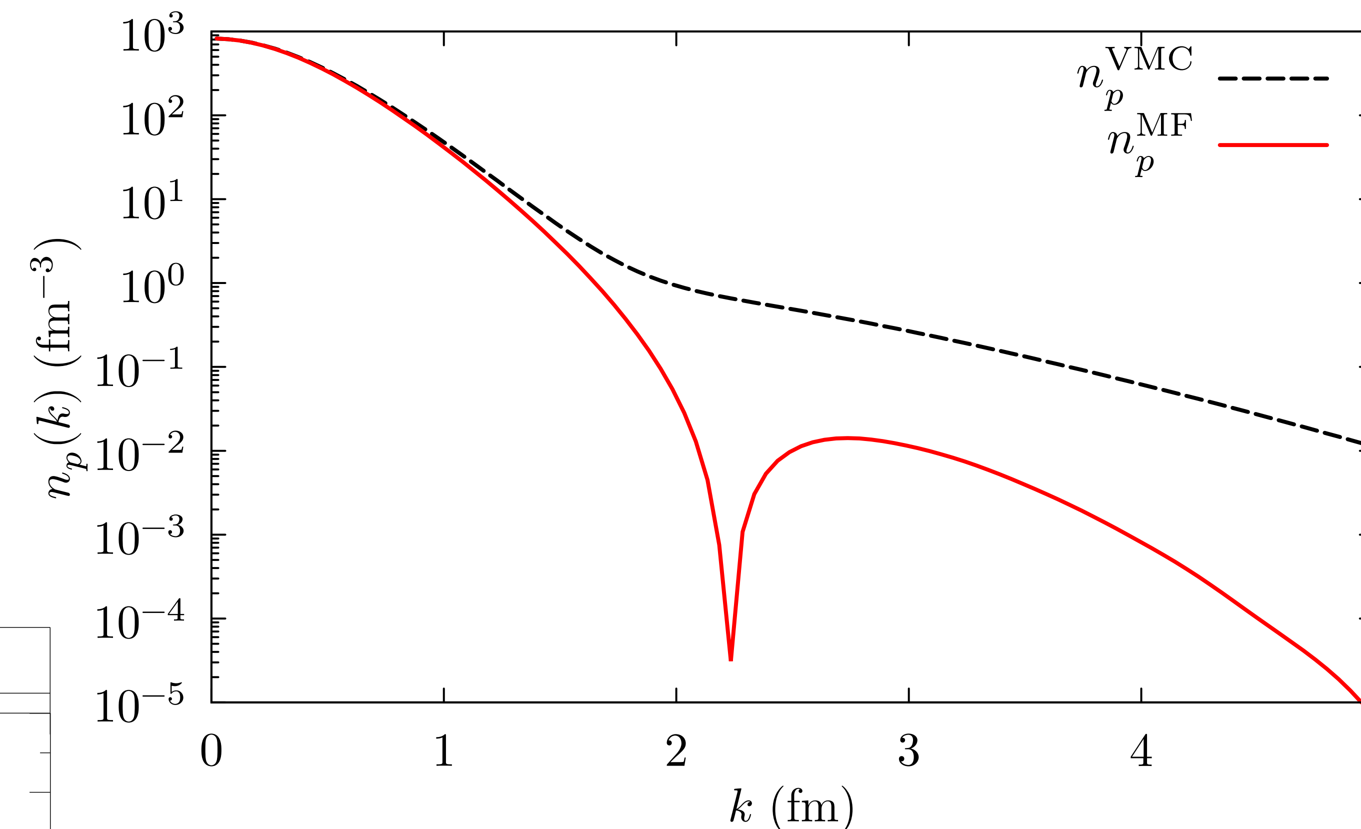

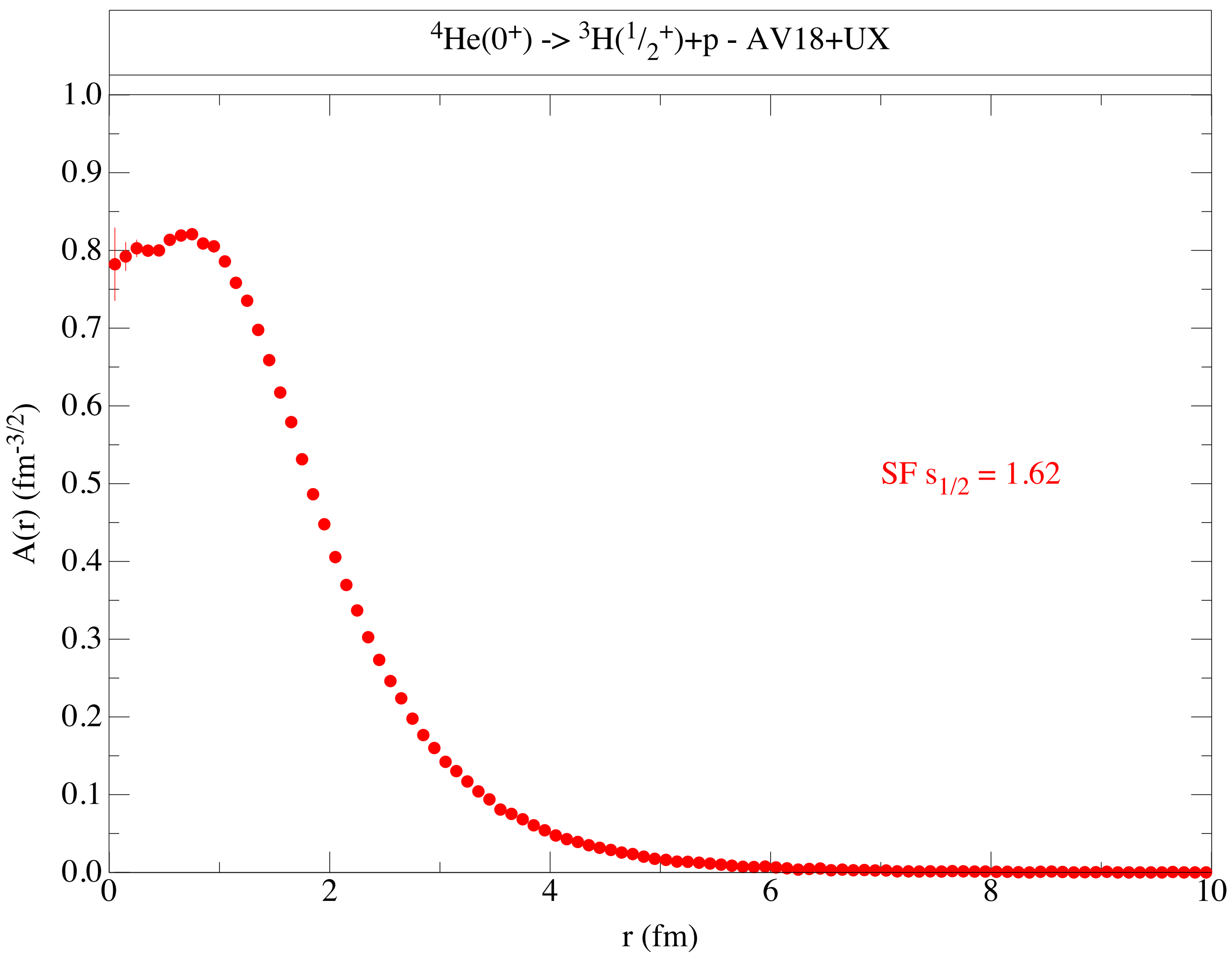

$$P_p^{\mathrm{MF}}(\mathbf{k}, E) = n_p^{\mathrm{MF}}(\mathbf{k}) \delta\left(E - B_{^4\mathrm{He}} + B_{^3\mathrm{H}} - \frac{k^2}{2m_{^3\mathrm{H}}}\right)$$

$$|\langle \Psi_0^{^4\mathrm{He}} | [|k\rangle \otimes |\Psi_0^{^3\mathrm{H}}\rangle]|^2$$

- The single-nucleon overlap has been computed within VMC (center of mass motion fully accounted for)

Noemi Rocco, nrocco@fnal.gov

Spectral function approach

$$P_p^{\rm corr}(\mathbf{k},E)=\sum_n\int\frac{d^3k'}{(2\pi)^3}|\langle\Psi_0^A|[|k\rangle\,|k'\rangle\,|\Psi_n^{A-2}\rangle]|^2\delta(E+E_0^A-e(\mathbf{k}')-E_n^{A-2})$$

Using QMC techniques

$$\sum_{\tau_{k'}=p,n}n_{p,\tau_{k'}}(\mathbf{k},\mathbf{k}')\delta\Big(E-B_A\quad-e(\mathbf{k}')+B_{A-2}-\frac{(\mathbf{k}+\mathbf{k}')^2}{2m_{A-2}}\Big)$$

Only SRC pairs should be considered: $|\Psi_0^{A-1}\rangle$ and $|k'\rangle|\psi_n^{A-2}\rangle$ be orthogonalized

One can introduce **cuts** on the **relative distance** between the particles in the two-body momentum distribution

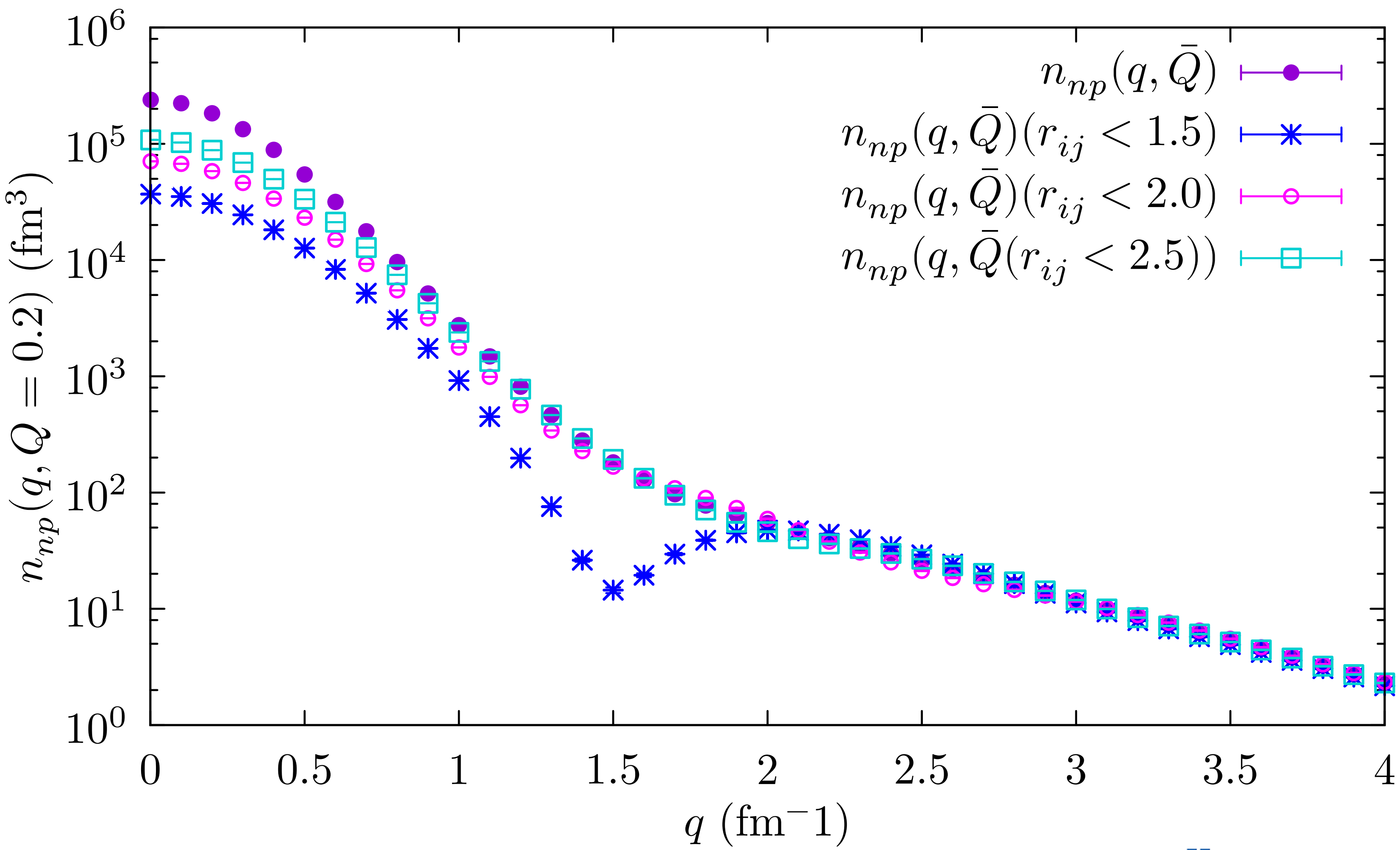

Noemi Rocco, nrocco@fnal.gov

QMC Spectral Function of ^{12}C

- The p-shell contribution has been obtained by FT the radial overlaps:

$$^{12}\mathrm{C}(0^+) \rightarrow ^{11}\mathrm{B}(3/2^-) + p$$
$$^{12}\mathrm{C}(0^+) \rightarrow ^{11}\mathrm{B}(1/2^-) + p$$
$$^{12}\mathrm{C}(0^+) \rightarrow ^{11}\mathrm{B}(3/2^-)^* + p\,.$$

R. Crespo, et al, Phys.Lett.B 803 (2020) 135355

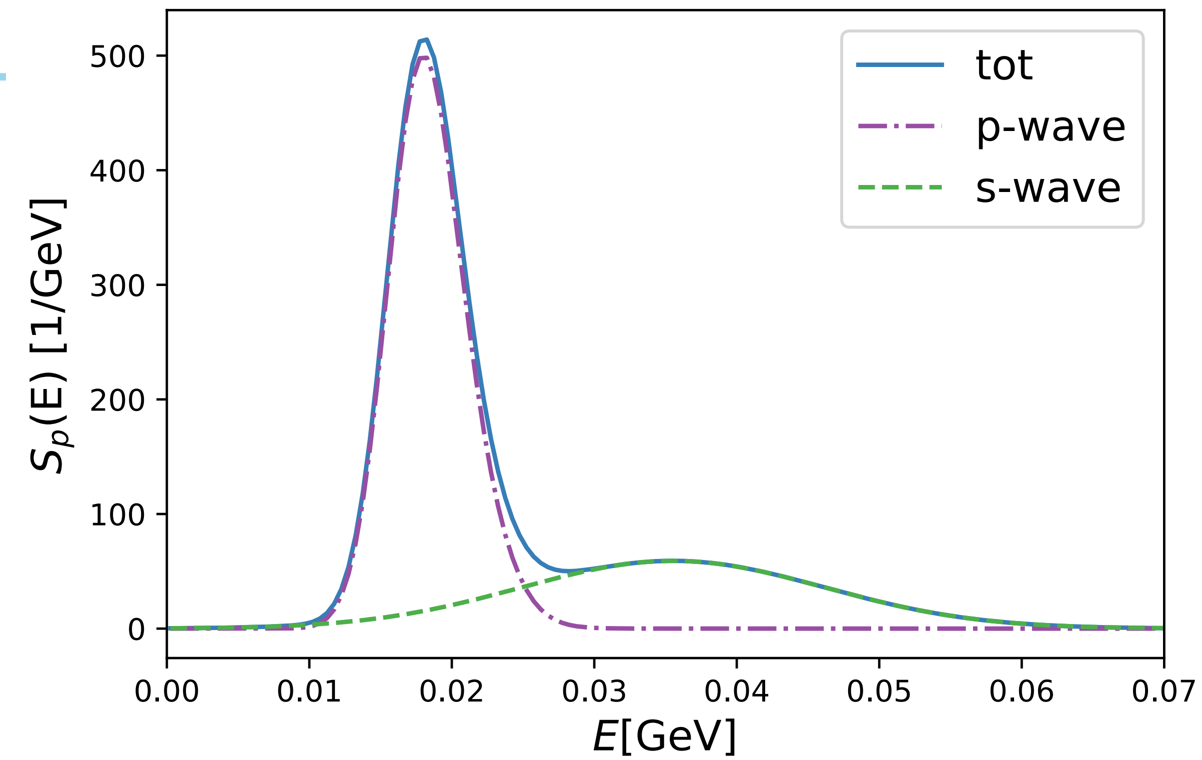

- The quenching of the spectroscopic factors automatically emerges from the VMC calculations

Computing the s-shell contribution is non trivial within VMC. We explored different alternatives:

- Quenched Harmonic Oscillator
- Quenched Wood Saxon
- VMC overlap associated for the $^4\mathrm{He}(0^+) \rightarrow\ ^3\mathrm{H}(1/2^+) + p$ transition

Korover, et al, CLAS collaboration PRC 107 (2023) 6, L061301

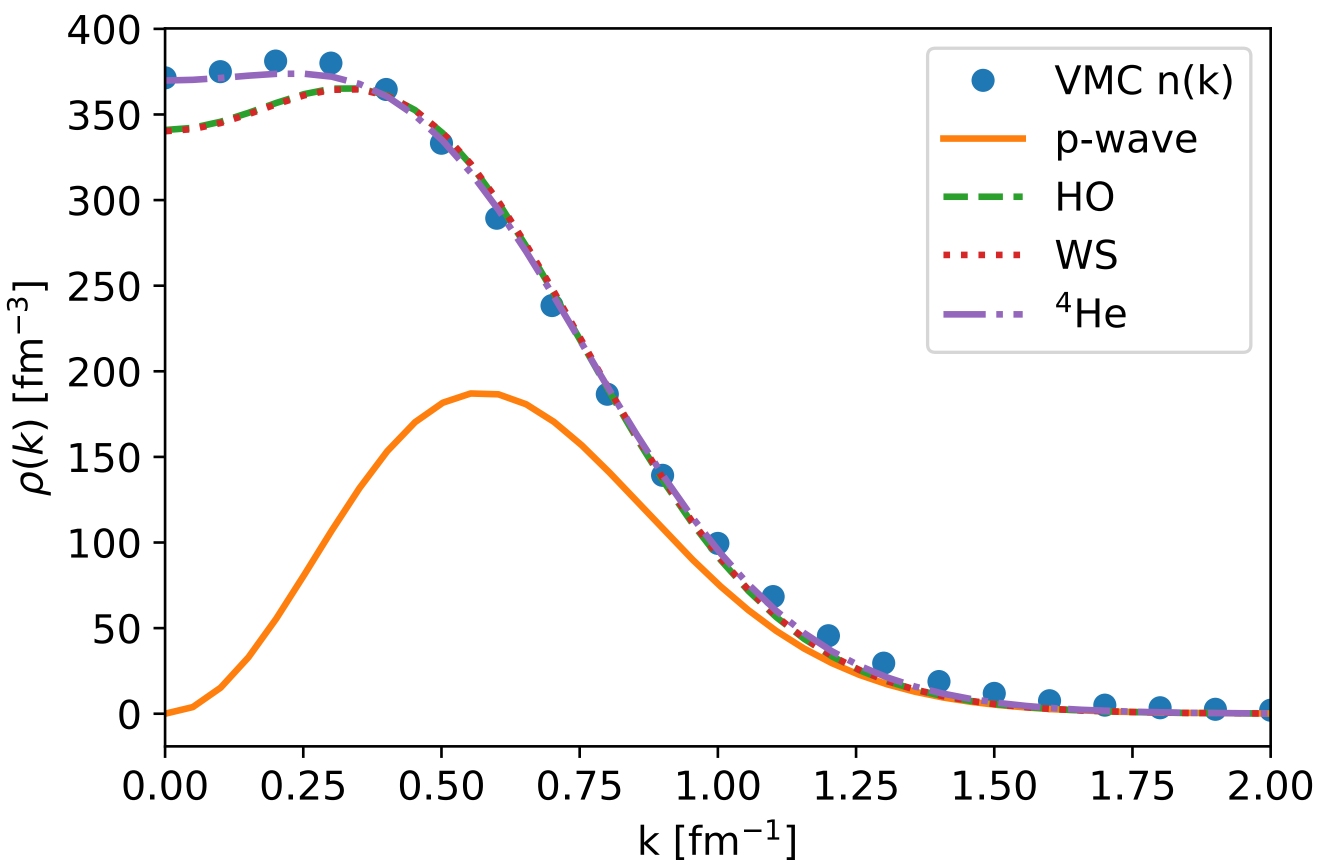

Noemi Rocco, nrocco@fnal.gov

Study of model dependence in neutrino predictions

Percent change in the MiniBooNE cross section versus the percent change in the two-body current parameters for 0.5 < cos θμ < 0.6, Tμ = 325 MeV

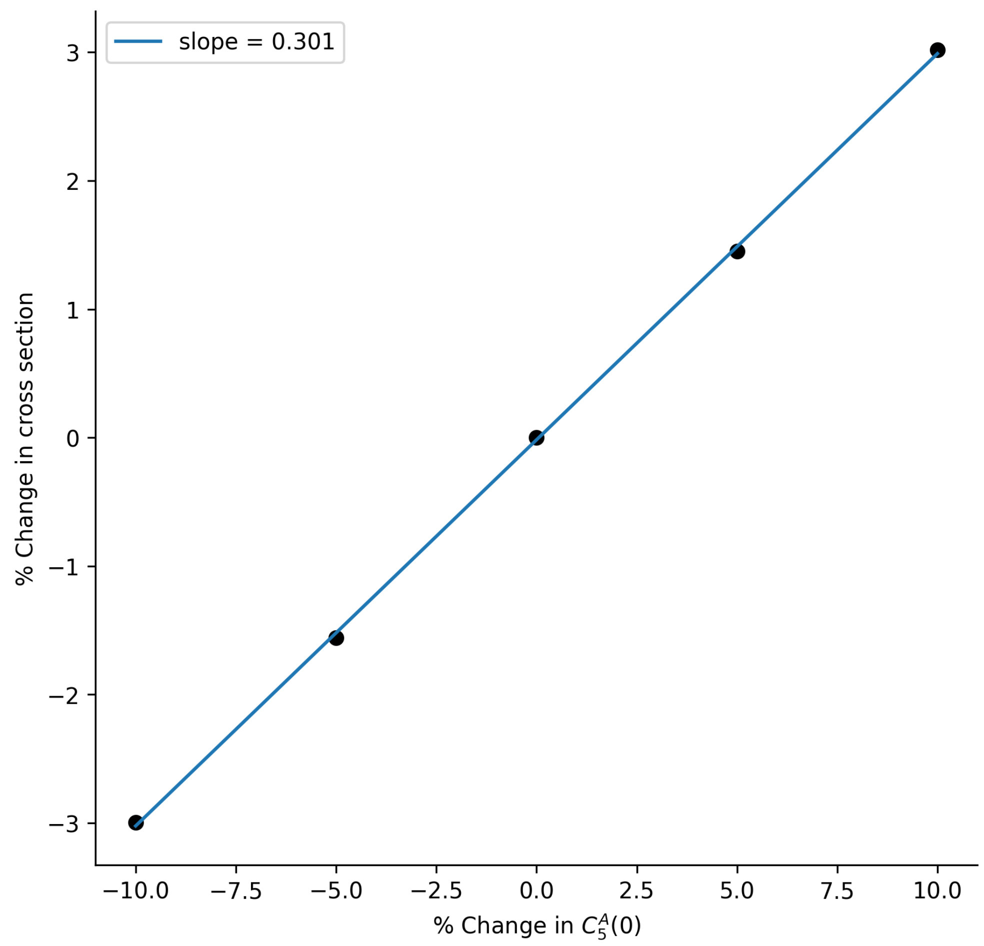

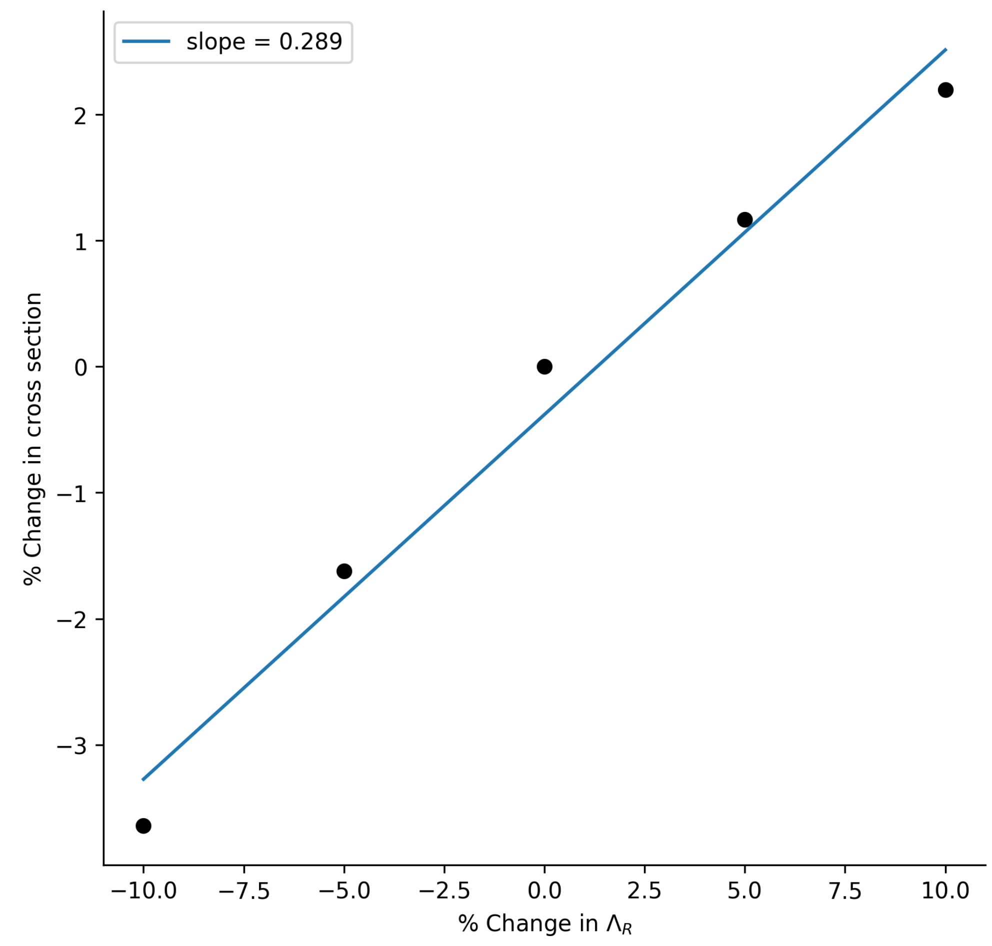

A 15% variation in either $C_5^A(0)$ or Λ_R changes the flux-averaged cross section by roughly 5%

Noemi Rocco, nrocco@fnal.gov

Two-body currents - Delta contribution

Rarita-Schwinger propagator

$$G^{\alpha\beta}(p_\Delta) = \frac{P^{\alpha\beta}(p_\Delta)}{p_\Delta^2 - M_\Delta^2}$$

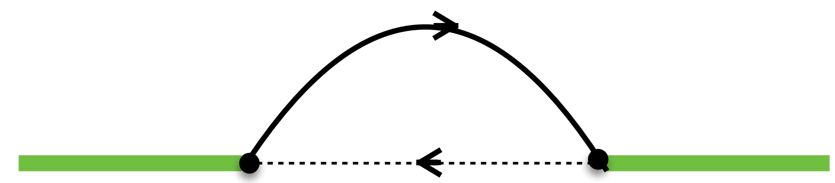

The spin 3/2 projection operator reads

$$P^{\alpha\beta}(p_\Delta) = (\not{p}_\Delta + M_\Delta)\left[g^{\alpha}\beta - \frac{1}{3}\gamma^\alpha\gamma^\beta - \frac{2}{3}\frac{p_\Delta^\alpha p_\Delta^\beta}{M_\Delta^2} + \frac{1}{3}\frac{p_\Delta^\alpha\gamma^\beta - p_\Delta^\beta\gamma^\alpha}{M_\Delta}\right].$$

To account for the resonant behavior of the Δ: $M_\Delta \to M_\Delta - i\Gamma(p_\Delta)/2$

$$\Gamma(p_\Delta) = -2\mathrm{Im}\Sigma_{\pi\mathrm{N}}(\mathrm{s}) = \frac{(4\mathrm{f}_{\pi\mathrm{N}\Delta})^2}{12\pi\mathrm{m}_\pi^2}\frac{|\mathbf{d}|^3}{\sqrt{\mathrm{s}}}(\mathrm{m_N} + \mathrm{E_d})\mathrm{R}(\mathbf{r}^2)$$

d is the decay three-momentum in the πN center of mass frame

In medium effects of the Δ $\Gamma_\Delta(p_\Delta) \to \Gamma_\Delta(p_\Delta) - 2\mathrm{Im}[\mathrm{U}_\Delta(\mathrm{p}_\Delta, \rho = \rho_0)]$

Noemi Rocco, nrocco@fnal.gov

Comparing different many-body methods

- e -^{3}H: inclusive cross section

L. Andreoli, NR, et al, PRC 105 (2022) 1, 014002

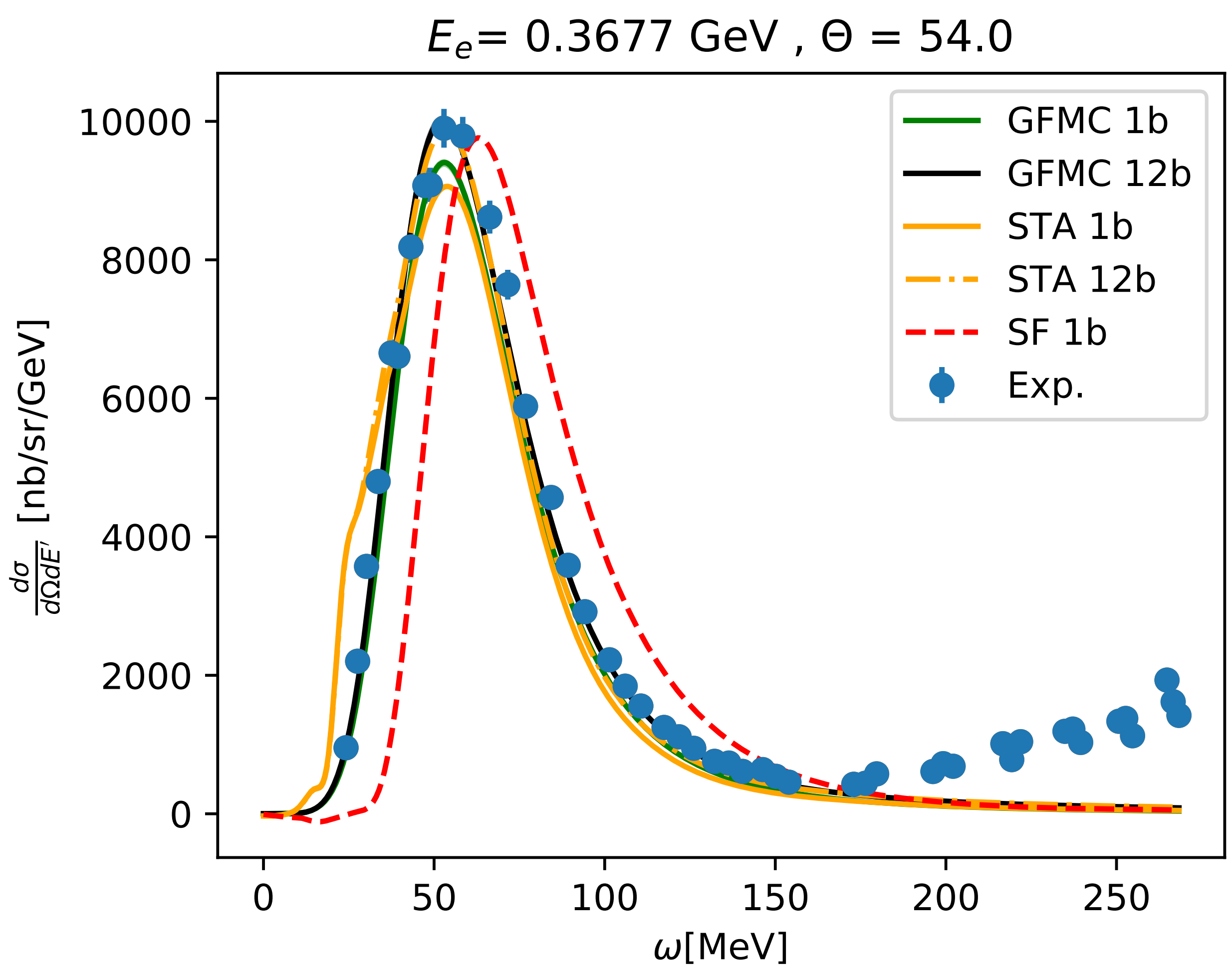

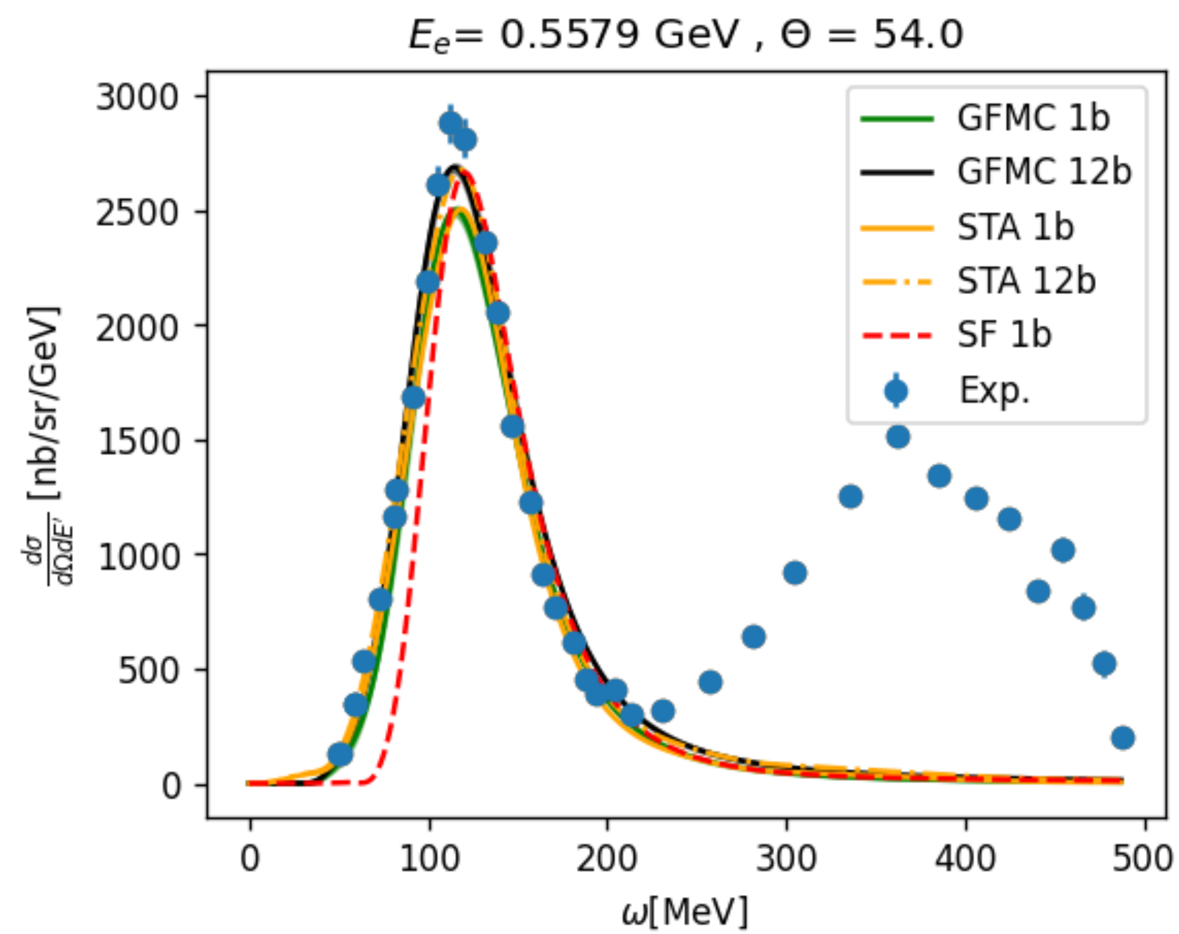

- Comparisons among QMC, SF, and STA approaches: first step to precisely **quantify the uncertainties i**nherent to the factorization of the final state.

- Gauge the role of **relativistic effects** in the energy region relevant for neutrino experiments.

Noemi Rocco, nrocco@fnal.gov

Green's Function Monte Carlo

Any trial wave function can be expanded in the complete set of eigenstates of the the Hamiltonian according to

$$|\Psi_V\rangle = \sum_n c_n |\Psi_n\rangle \qquad\qquad H|\Psi_n\rangle = E_n|\Psi_n\rangle$$

GFMC uses a projection technique to **enhance the true ground-state component** of a starting wave function.

$$\lim_{\tau\to\infty} e^{-(H-E_0)\tau}|\Psi_T\rangle = \lim_{\tau\to\infty}\sum_n c_n\, e^{-(E_n-E_0)\tau}|\Psi_n\rangle = c_0|\Psi_0\rangle$$

The direct calculation of the imaginary-time propagator for strongly-interacting systems involves prohibitive difficulties

J. Carlson , et al. Rev. Mod. Phys. 87 (2015) 1067

The imaginary-time evolution is broken into N small imaginary-time steps, and complete sets of states are inserted

$$e^{-(H-E_0)\tau}|\Psi_V\rangle = \int dR_1 \dots dR_N |R_N\rangle\langle R_N|e^{-(H-E_0)\Delta\tau}|R_{N-1}\rangle \dots \langle R_2|e^{-(H-E_0)\Delta\tau}|R_1\rangle\Psi_V(R_1)$$

Short Time Propagator

Noemi Rocco, nrocco@fnal.gov

Phenomenological potential: av18 + IL7

Phenomenological potentials explicitly include the **long-range one-pion exchange interaction** and a set of **intermediate- and short-range phenomenological terms**

- **Argonne v18** is a finite, local, configuration-space potential controlled by ~4300 np and pp scattering data below 350 MeV of the Nijmegen database

$$v_{ij} = \sum_{p=1}^{18} v^p(r_{ij}) O^p_{ij} \quad \longleftrightarrow$$

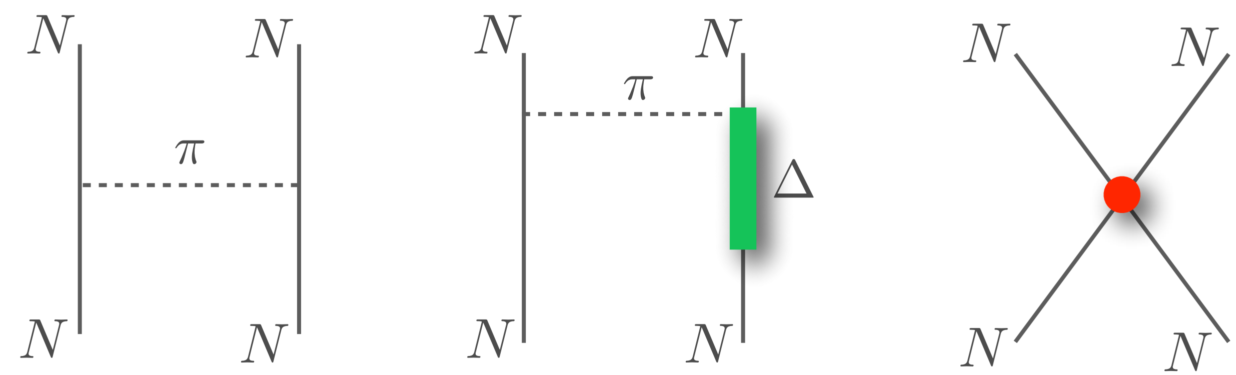

- Phenomenological three-nucleon interactions, like the **Illinois 7**, effectively include the lowest nucleon excitation, the Δ(1232) resonance, end other nuclear effects

$$V^{3\mathrm{N}}_{ijk} = A^{PW}_{2\pi} O^{2\pi,PW}_{ijk} + A^{SW}_{2\pi} O^{2\pi,SW}_{ijk} + A^{\Delta R}_{3\pi} O^{3\pi,\Delta R}_{ijk} + A^{R} O^{R}_{ijk} \quad \longleftrightarrow$$

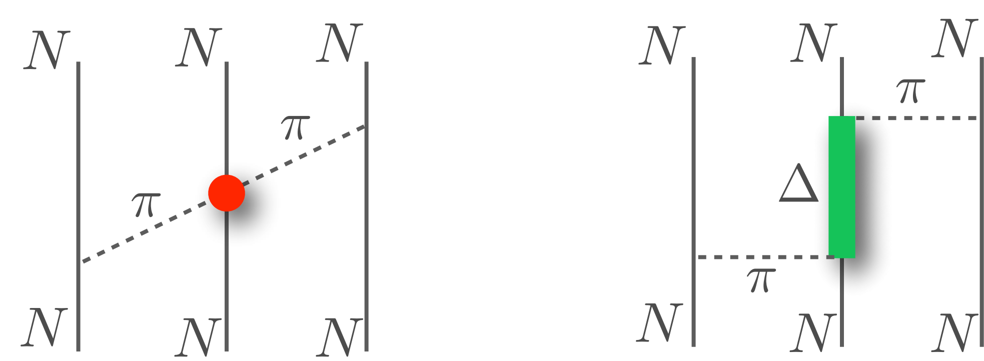

The parameters of the AV18 + IL7 are fit to properties of **exactly solvable light nuclear systems**.

Noemi Rocco, nrocco@fnal.gov

Axial form factor determination

- The axial form-factor has been fit to the dipole form

$$F_A(q^2) = \frac{g_A}{(1 - q^2/m_A^2)^2}$$

- The intercept g_A=-1.2723 is known from neutron β decay

- Different values of m_A from experiments
  - m_A =1.02 GeV q.e. scattering from deuterium
  - m_A =1.35 GeV @ MiniBooNE

- Alternative derivation based on **z-expansion** —model independent parametrization

$$F_A(q^2) = \sum_{k=0}^{k_{\max}} a_k z(q^2)^k,$$

known functions

free parameters

Bhattacharya, Hill, and Paz PRD 84 (2011) 073006

A.S.Meyer et al, Phys.Rev.D 93 (2016) 11, 113015

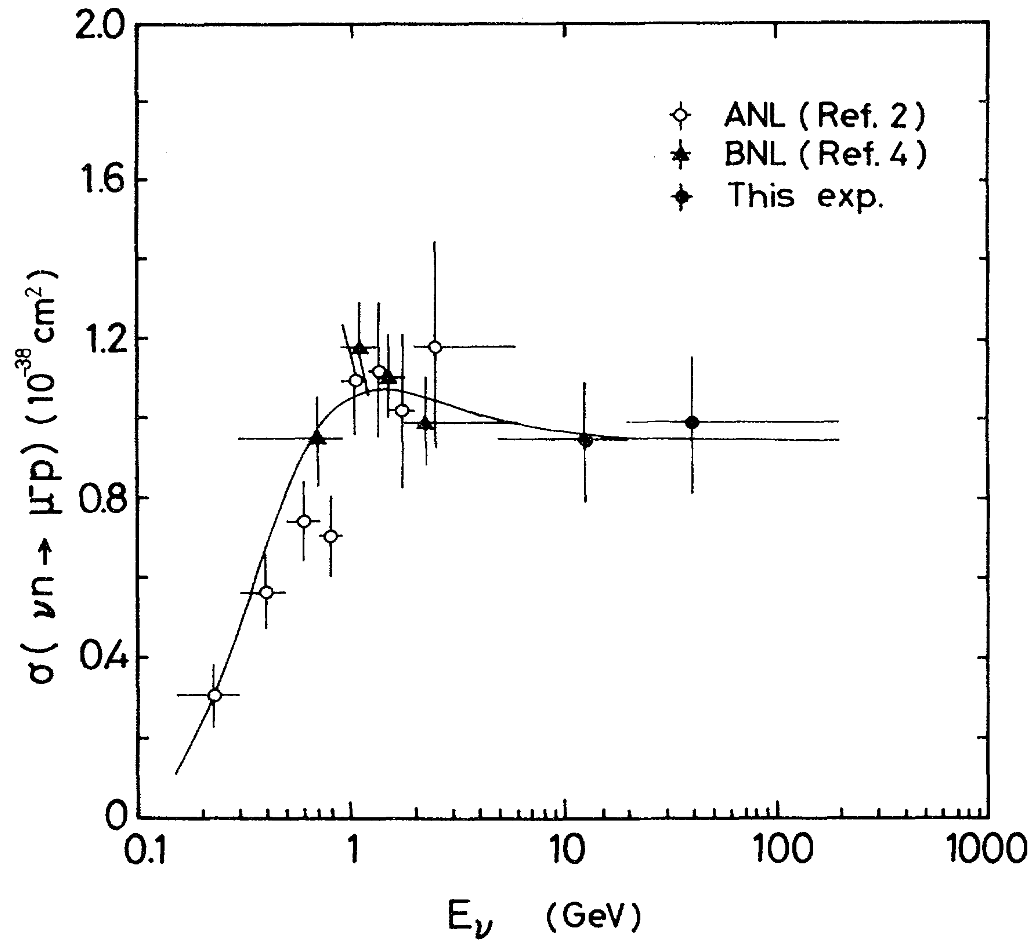

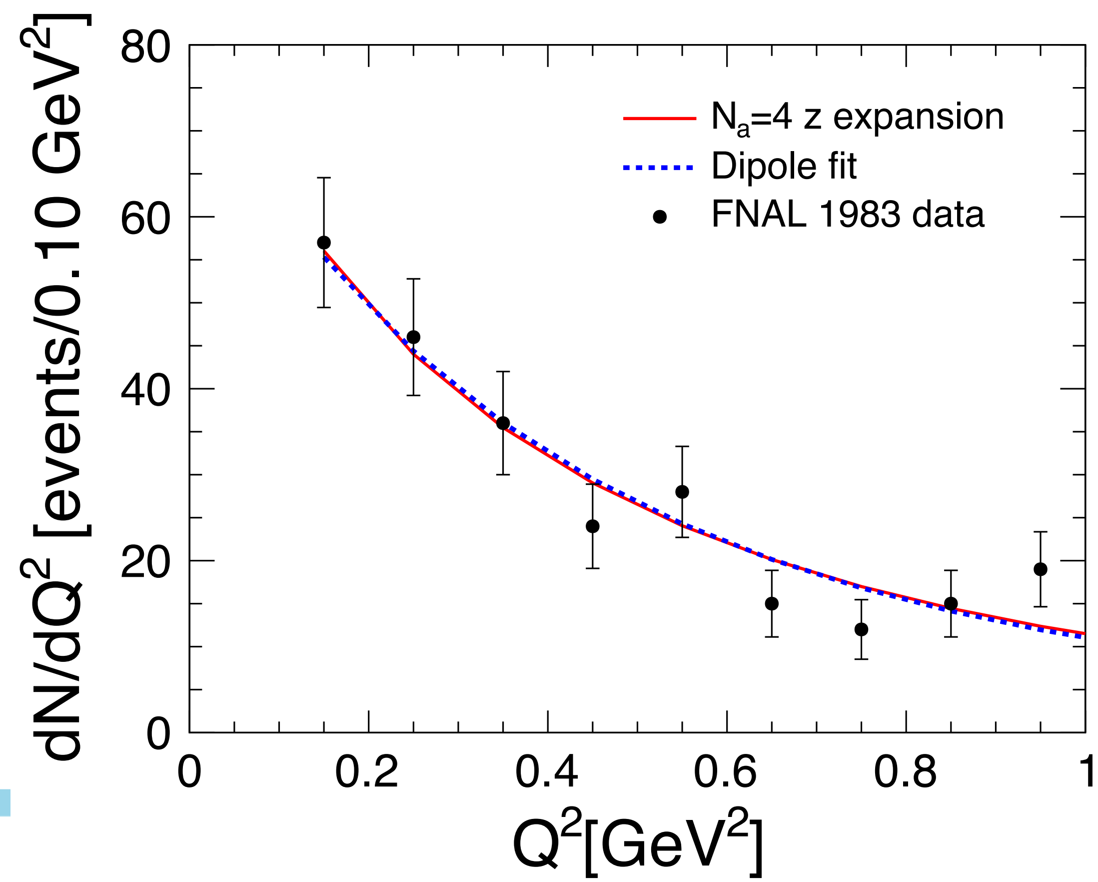

Neutrino-Nucleon scattering

- Sum rule can be enforced ensuring that the form factor falls smoothly to zero at large Q^2

$$\sum_{k=n}^{\infty} k(k-1)\cdots(k-n+1)a_k = 0\,, \quad n = 0,1,2,3$$

Fit deuteron data replacing dipole axial form factor with z-expansion, enforce the sum rule constraints

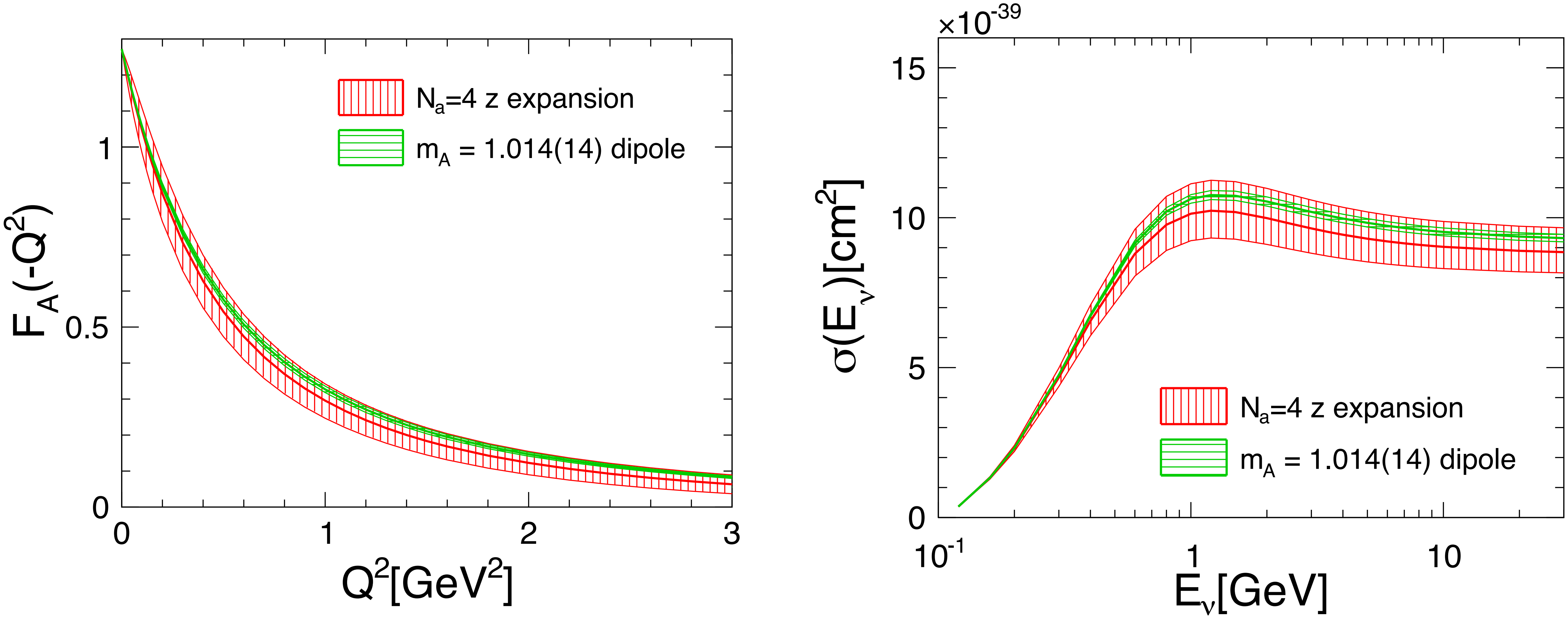

A.S.Meyer, Phys.Rev.D 93 (2016) 11, 113015